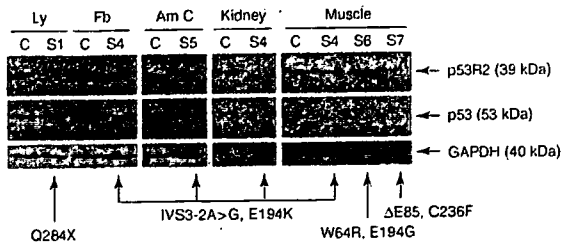

Figure 4 Protein blot analysis. Ly, lymphoblastoid cell lines; Fb, fibroblasts; Am C, amniotic cells; C, control; S1–S7, subjects 1–7. Overexposure showed trace amounts of p53R2 protein in muscle of subject 7. The lower bands for p53R2 and GAPDH observed in kidney of subject 4 might be related to abnormal migration due to immersion of the biopsy in Tissue-Tek OCT compound for histological studies. The protein alterations are indicated for each subject.

Protein blot analyses showed that p53R2 was undetectable in lymphoblastoid cell lines from subject 1 and barely detectable in muscle of subject 7 (**Fig. 4**). Subjects 4 and 5 had a reduced level of the protein in cultured skin fibroblasts, amniotic cells and/or kidney but not in muscle, whereas no quantitative or qualitative modification could be observed in muscle of subject 6. Finally, we observed an induction of p53 protein in primary cultured fibroblasts from subject 4 and in amniotic cells from subject 5, whereas control cultured cells were devoid of p53. Both control and subject 1 lymphoblastoid cell lines expressed p53, roughly equally, a feature of transformed cells. As *Rrm2b* inactivation in mouse resulted in an increase of apoptotic cells in kidney, we studied the expression of Bax and Bcl2 in cells from affected humans and observed a slight decrease of Bcl2 protein in lymphoblastoid cell lines from subject 1, indicating that there may be an increase in apoptosis in these cells as well (**Supplementary Fig. 3** on line). No Bcl2 expression could be detected in fibroblasts of subject 4 and amniotic cells of subject 5.

RRM2B was previously identified as a target of p53, and its induction following DNA damage was believed to result in urgently needed dNTPs synthesis for DNA repair, as R2 is absent during the G_0/G_1 phase. Yet *RRM2B* is not only induced by p53 following DNA damage: it is also constitutively expressed in proliferative and nonproliferative tissues, allowing a low but constant dNTPs synthesis throughout the cell cycle[14,15]. The observation of a severe mtDNA depletion caused by mutations in *RRM2B* demonstrates that p53R2 has a crucial role in dNTPs supply, especially for the synthesis of mtDNA, which constantly replicates. The *RRM2B* gene is ubiquitously expressed in human, with high expression in skeletal muscle. By contrast, transcripts encoding R2 are undetectable in heart, brain and muscle, implying that these tissues entirely rely on p53R2 for dNTPs synthesis, whereas a low but significant amount of R2 is detected in kidney[16]. Why *RRM2B* mutations resulted only in severe neurological and/or renal involvement remains an open question. Other mechanisms, including post-translational modifications of p53R2 or R2 or post-transcriptional modifications of their respective mRNAs, could help explain the tissue-specific phenotype of *RRM2B* mutations.

The $Rrm2b^{-/-}$ mouse presents a milder phenotype than humans with *RRM2B* mutations. This is likely to be related to the relatively low expression of the *Rrm2b* gene in mouse tissues[8] compared with human[16]. The study of other ribonucleotide reductase subunits in $Rrm2b^{-/-}$ mouse tissues could allow one to investigate these phenotypic differences. Despite showing only slight impairment, $Rrm2b^{-/-}$ mice show a substantial decrease of mtDNA copy number but no obvious respiratory chain defect. One might hypothesize that the threshold in mtDNA content for expression of a respiratory chain defect differs between mouse and human and also among different tissues. Indeed, a reduction to 4% of normal mtDNA content in liver of the $Mpv17^{-/-}$ mouse results in a respiratory chain defect[5], whereas a reduction to 6% in muscle of the $Rrm2b^{-/-}$ mouse does not.

Whether the induction of p53 observed in cultured cells from affected individuals results specifically from *RRM2B* mutation, or more generally from mtDNA depletion and respiratory chain dysfunction, remains to be investigated. We note that p53 is also expressed exclusively in collecting tubules in the medulla of the kidney of $Rrm2b^{-/-}$ mouse, implying that there may be a common mechanism in human cells and some mouse tissues[8]. Nevertheless, this response suggests that *p53* is involved not only in the suppression of tumor development following DNA injury but also in other, as yet unknown functions during cell life, including mitochondrial control, as implied by the recently discovered regulation of aerobic respiration by p53 by way of *SCO2* expression[17]. It is now well established that nuclear gene expression responds to mitochondrial dysfunction elicited by a mitochondria-to-nucleus signaling pathway, called retrograde regulation. Retrograde signaling in yeast involves the RTG (for 'retrograde') pathway[18], whereas in mammals, it occurs through increased cytosolic Ca^{2+} or activation of NFκB[19]. One could hypothesize that p53 also contributes to this retrograde signaling, at least in the case of *RRM2B* mutations.

METHODS

Subjects. Subjects 1–3 were born to consanguineous Moroccan parents after normal pregnancy (**Fig. 1**). Subject 1 showed trunk hypotonia and lactic acidosis in the first month of life. She also developed proximal tubulopathy. Her neurological condition suddenly worsened at 6 weeks of age with a severe lactic acidosis (5.5 mM; control values < 2 mM) and she died at 2 months of age. The two other sibs followed a similar course. Respiratory chain analysis showed a severely decreased malate+glutamate oxidation and a complex IV deficiency in muscle of subject 1, whereas cultured skin fibroblasts from subject 2 were normal (**Table 1**). Severe mtDNA depletion was found in muscle of subject 3 (1% of control mtDNA content; **Fig. 2**). Subjects 4 and 5 were born to healthy unrelated parents of French origin after a normal pregnancy and delivery (**Fig. 1**). Subject 4, a boy, showed trunk hypotonia and tubulopathy shortly after birth. At 20 days of life, he developed seizures with high plasma (6.5 mM; control values < 2 mM) and CSF (3.3 mM; control values < 2 mM) lactate. He died at 2 months of age after status epilepticus. His sister, subject 5, showed neonatal hyperlactatemia. Her clinical course was similar to that of her brother and she died at 2 months of age. Skeletal muscle biopsies of these two subjects showed a combined complex I, III and IV deficiency, whereas cultured skin fibroblasts of subject 4 showed only a decreased complex III activity (**Table 1**). Only 2% of the normal mtDNA content was detected in muscle of subject 4 (**Fig. 2**). Subject 6 has been previously reported[20] (**Fig. 1**). Soon after birth she showed hypotonia; she developed respiratory distress, hyperlactatemia and tubulopathy at 3 months of age. She died at 4 months of age. Subject 7 was a girl, born to unrelated healthy parents of French origin (**Fig. 1**). She had neonatal trunk hypotonia and she rapidly developed vomiting and diarrhea with high plasma (6.79 mM; control values < 2 mM) and CSF (3.5 mM; control values < 2 mM) lactate. She died at 3 months of age. Muscle histology showed ragged red fibers and histoenzymological studies showed cytochrome oxidase deficiency. The activities of complexes I, III and IV in her muscle were severely decreased (**Table 1**) and muscle mtDNA content averaged 1% of controls (**Fig. 2**). All procedures were approved by the review board of the Necker Hospital. We obtained informed consents from parents of all probands and sibling before collecting blood for DNA extraction or performing tissue biopsies.

Lod score analysis. We performed SNP genotyping using the GeneChip Human Mapping 10K Array Xba 142 2.0. For parametric multipoint

Table 1 Respiratory chain activities in muscle homogenate, muscle mitochondria and cultured skin fibroblasts of subjects and controls

	Muscle mitochondria			Muscle homogenate			Fibroblasts		
	S1	S7	Control	S4	S5	Control	S4	S7	Control
	Activities (nmol/min per mg protein)								
Mal+pyr ox		15	31.3 ± 8.9						
Mal+glu ox	2		28.7 ± 10.7						
Succinate ox	42	25.2	55.5 ± 15.9						
CI		28.8	65.7 ± 16.7	3	7	18.4 ± 4.7	35	48.2	35.2 ± 9.4
CII		302.6	98.9 ± 26.4	389	76	33.6 ± 7.9	64	100.4	67 ± 15.9
CIII		272.2	1,257.9 ± 319.9	56	76	354.5 ± 74.3	394	1,208.2	718.3 ± 179.5
CIV	397	146.9	731.1 ± 231.5	18	29	154.1 ± 37.7	349	537.2	352.5 ± 86.9
CV		273.7	255.9 ± 77.7	113	364	159.4 ± 43.4	77	75.8	109.7 ± 77.7
CII+III	755	221.3	228.2 ± 62.8				99	219.7	227 ± 49.7
CS		795	364.8 ± 92.3	433	202	111.2 ± 23.8	162	367.1	932.0 ± 264.9
	Activity ratios								
CIV/CI		5.1	10.7 ± 1.9	6.7	4.1	9.2 ± 1.1	10.0	11.1	10.0 ± 1.5
CIV/CII		0.48	8.0 ± 0.7	0.0	0.4	5.3 ± 0.2	5.5	5.3	6.6 ± 1.0
CIV/CIII		0.54	0.5 ± 0.04	0.3	0.4	0.5 ± 0.04	0.9	0.4	0.6 ± 0.006
CIV/CV		0.53	2.4 ± 0.3	0.2	0.1	1.2 ± 0.1	4.5	7.1	3.1 ± 0.5
CIV/CII+III	0.5	0.66	3.4 ± 0.9				3.5	2.4	3.9 ± 0.4

S1–S7, subjects 1–7; mal+pyr, malate + pyruvate; mal+glu, malate + glutamate; ox, oxidation; CI–CIV, complexes I–IV of the respiratory chain; CS, citrate synthase. Control values are mean ± s.d.

analysis, we used Merlin 1.01 software[21] assuming complete penetrance of the recessive disorder.

Sequence analysis. We amplified exons of the *RRM2B* gene using specific primers (**Supplementary Table 1** online) with an initial denaturation at 96 °C for 5 min, followed by 30 cycles of 96 °C for 30 s, 55 °C for 30 s and 72 °C for 30 s, and a final extension at 72 °C for 10 min.

Biochemical assays. We carried out polarographic tests and spectrophotometric assays of respiratory chain enzymes on human and mouse skeletal muscle mitochondria, muscle, liver and kidney homogenates as previously described[22].

Cell cultures. Lymphoblastoid cell lines and skin fibroblasts were grown in RPMI1640 Glutamax (Invitrogen) + 10% fetal calf serum (decomplemented for lymphoblastoid cell lines), 50 μg/ml uridine, 2.5 mM sodium pyruvate, 200 U/ml penicillin and 200 U/ml streptomycin, at 37 °C in a 5% CO_2 atmosphere. For amniotic cells, we substituted OptiMEM (Invitrogen) for RPMI1640.

Protein blot analyses. We prepared total cellular protein extracts (40 μg) from frozen tissues (50–100 mg) or cultured cells (3×10^6 cells) as previously described and analyzed them by SDS-PAGE using a 10% acrylamide gel. The p53R2, p53 and GAPDH proteins were detected using specific antibodies. We purchased polyclonal antibodies to p53R2 and to GAPDH from Abcam. Antibody to p53 was purchased from Santa Cruz, and antibodies to Bcl2 and to Bax from Euromedex.

mtDNA quantification. We measured human and mouse mtDNA by quantitative real-time PCR as previously described[5,23]. For mouse mtDNA quantification, we used the mitochondrial *mt-Co1* and nuclear *Pde6b* genes (**Supplementary Table 1**).

Protein modeling. We modeled the three dimensional structure of the human p53R2 protein by comparative methods and energy minimization using the program SWISS-MODEL[24] in the optimized mode. The 2.8-Å coordinate set for the crystal structure of human R2 (PDB code 2IYH) served as the template for modeling the human p53R2 subunit. Residues 35–317 of the submitted sequence were used to build the model. Whatcheck analysis[25] confirmed the quality of the model. We used Swiss-Pdb Viewer 3.7 (ref. 26) to visualize the structures and gain structural insight into the p53R2 substitutions and deletions. For p53R2 homodimeric docking, we used the *ClusPro* Web Server software[9,10], using the modeled three-dimensional structure of the human p53R2 subunit.

Accession numbers. R1, ribonucleoside-diphosphate reductase M1 chain (*Homo sapiens*), NP_001024. R2, ribonucleotide reductase M2 polypeptide (*Homo sapiens*), NP_001025. p53R2 protein, ribonucleotide reductase (TP53 inducible, *Homo sapiens*), NP_056528. *RRM2B* mRNA, NM_015713. *RRM2B* gene, AB036532. *mt-Co1* (*Mus musculus*), NC_005089. *Pde6b*, phosphodiesterase 6B, cyclic GMP, rod receptor, β polypeptide (*Mus musculus*), AC158912. *E. coli* R1, Protein Data Bank 4R1R.

Note: Supplementary information is available on the Nature Genetics website.

ACKNOWLEDGMENTS

We thank T. Soussi for discussion and J. Bentata, B. Chabrol, C. Fallet-Bianco and J.M. Liet for referring the study subjects. This research was supported in part by the Association Française contre les Myopathies, Mitocircle European Union Project (contract number LSHB-CT-2004-005260), Eumitocombat within the European Union Sixth Framework Program for Research, Priority 1 'Life sciences, genomics and biotechnology for health' (contract number LSHM-CT-2004-503116) and the French Agence Nationale pour la Recherche.

AUTHOR CONTRIBUTIONS

A.B. identified the *p53R2* mutations and performed the protein blot and mtDNA quantification in mouse, L.M. performed protein blot analysis, V.S. performed the modeling of ribonucleotide reductase, J.-P.J. performed the linkage analysis using Merlin software, E.S. performed the mitochondrial DNA quantification, S.A. was in charge of cell culture, D.C. identified the respiratory chain enzyme activity, P.d.L. was responsible for clinical management of subjects 3, 4 and 7 and their diagnosis, V.P.-F. was responsible for clinical management of subject 7 and her diagnosis, H.A. and Y.N. produced the *Rrm2b*$^{-/-}$ mouse, A.M. was responsible for clinical management of subjects 1 and 2 and wrote the paper, and A.R. designed the project and wrote the paper.

COMPETING INTERESTS STATEMENT

The authors declare no competing financial interests.

Published online at http://www.nature.com/naturegenetics
Reprints and permissions information is available online at http://npg.nature.com/reprintsandpermissions

1. Ferrari, G. *et al.* Infantile hepatocerebral syndromes associated with mutations in the mitochondrial DNA polymerase-γA. *Brain* **128**, 723–731 (2005).
2. Mandel, H. *et al.* The deoxyguanosine kinase gene is mutated in individuals with depleted hepatocerebral mitochondrial DNA. *Nat. Genet.* **29**, 337–341 (2001).
3. Saada, A. *et al.* Mutant mitochondrial thymidine kinase in mitochondrial DNA depletion myopathy. *Nat. Genet.* **29**, 342–344 (2001).
4. Elpeleg, O. *et al.* Deficiency of the ADP-forming succinyl-CoA synthase activity is associated with encephalomyopathy and mitochondrial DNA depletion. *Am. J. Hum. Genet.* **76**, 1081–1086 (2005).
5. Spinazzola, A. *et al. MPV17* encodes an inner mitochondrial membrane protein and is mutated in infantile hepatic mitochondrial DNA depletion. *Nat. Genet.* **38**, 570–575 (2006).
6. Nordlund, P. & Reichard, P. Ribonucleotide reductases. *Annu. Rev. Biochem.* **75**, 681–706 (2006).
7. Tanaka, H. *et al.* A ribonucleotide reductase gene involved in a p53-dependent cell-cycle checkpoint for DNA damage. *Nature* **404**, 42–49 (2000).
8. Kimura, T. *et al.* Impaired function of p53R2 in Rrm2b-null mice causes severe renal failure through attenuation of dNTP pools. *Nat. Genet.* **34**, 440–445 (2003).
9. Comeau, S.R., Gatchell, D.W., Vajda, S. & Camacho, C.J. ClusPro: a fully automated algorithm for protein-protein docking. *Nucleic Acids Res.* **32**, W96–W99 (2004).
10. Comeau, S.R., Gatchell, D.W., Vajda, S. & Camacho, C.J. ClusPro: an automated docking and discrimination method for the prediction of protein complexes. *Bioinformatics* **20**, 45–50 (2004).
11. Eklund, H., Uhlin, U., Farnegardh, M., Logan, D.T. & Nordlund, P. Structure and function of the radical enzyme ribonucleotide reductase. *Prog. Biophys. Mol. Biol.* **77**, 177–268 (2001).
12. Lycksell, P.O., Ingemarson, R., Davis, R., Graslund, A. & Thelander, L. 1H NMR studies of mouse ribonucleotide reductase: the R2 protein carboxyl-terminal tail, essential for subunit interaction, is highly flexible but becomes rigid in the presence of protein R1. *Biochemistry* **33**, 2838–2842 (1994).
13. Kolberg, M., Strand, K.R., Graff, P. & Andersson, K.K. Structure, function, and mechanism of ribonucleotide reductases. *Biochim. Biophys. Acta* **1699**, 1–34 (2004).
14. Hakansson, P., Hofer, A. & Thelander, L. Regulation of mammalian ribonucleotide reduction and dNTP pools after DNA damage and in resting cells. *J. Biol. Chem.* **281**, 7834–7841 (2006).
15. Chabes, A.L., Pfleger, C.M., Kirschner, M.W. & Thelander, L. Mouse ribonucleotide reductase R2 protein: a new target for anaphase-promoting complex-Cdh1-mediated proteolysis. *Proc. Natl. Acad. Sci. USA* **100**, 3925–3929 (2003).
16. Zhou, B. *et al.* The human ribonucleotide reductase subunit hRRM2 complements p53R2 in response to UV-induced DNA repair in cells with mutant p53. *Cancer Res.* **63**, 6583–6594 (2003).
17. Matoba, S. *et al.* p53 regulates mitochondrial respiration. *Science* **312**, 1650–1653 (2006).
18. Liu, Z. & Butow, R.A. Mitochondrial retrograde signaling. *Annu. Rev. Genet.* **40**, 159–185 (2006).
19. Butow, R.A. & Avadhani, N.G. Mitochondrial signaling: the retrograde response. *Mol. Cell* **14**, 1–15 (2004).
20. Paquis-Flucklinger, V. *et al.* Early-onset fatal encephalomyopathy associated with severe mtDNA depletion. *Eur. J. Pediatr.* **154**, 557–562 (1995).
21. Abecasis, G.R., Cherny, S.S., Cookson, W.O. & Cardon, L.R. Merlin—rapid analysis of dense genetic maps using sparse gene flow trees. *Nat. Genet.* **30**, 97–101 (2002).
22. Rustin, P. *et al.* Biochemical and molecular investigations in respiratory chain deficiencies. *Clin. Chim. Acta* **228**, 35–51 (1994).
23. Sarzi, E. *et al.* Mitochondrial DNA depletion is a prevalent cause of multiple respiratory chain deficiency in childhood. *J. Pediatr.* (in the press).
24. Schwede, T., Kopp, J., Guex, N. & Peitsch, M.C. SWISS-MODEL: an automated protein homology-modeling server. *Nucleic Acids Res.* **31**, 3381–3385 (2003).
25. Hooft, R.W., Vriend, G., Sander, C. & Abola, E.E. Errors in protein structures. *Nature* **381**, 272 (1996).
26. Guex, N. & Peitsch, M.C. SWISS-MODEL and the Swiss-PdbViewer: an environment for comparative protein modeling. *Electrophoresis* **18**, 2714–2723 (1997).

Oncogene (2007), 1-13

www.nature.com/onc

ORIGINAL ARTICLE

Monomeric but not trimeric clathrin heavy chain regulates p53-mediated transcription

K Ohmori[1,2,3], Y Endo[1,2], Y Yoshida[1,2], H Ohata[1,2], Y Taya[1,2] and M Enari[1,2]

[1]Radiobiology Division, National Cancer Center Research Institute, Chuo-ku, Tokyo, Japan; [2]SORST, Japan Science and Technology Agency (JST), Chuo-ku, Tokyo, Japan and [3]Department of Integrated Biosciences, Graduate School of Frontier Sciences, The University of Tokyo, Kashiwa, Chiba, Japan

Tumor suppressor p53 protein is the transcription factor responsible for various genes including DNA repair, growth arrest, apoptosis and antiangiogenesis. Recently, we showed that clathrin heavy chain (CHC), which was originally identified as a cytosolic protein regulating endocytosis, is present in nuclei and functions as a coactivator for p53. Here, we determined the detailed p53-binding site of CHC and a CHC deletion mutant containing this region (CHC833-1406) behaved as a monomer in cells. Monomeric CHC833-1406 still had a higher ability to transactivate p53 than wild-type CHC although this CHC mutant no longer had endocytic function. Moreover, similar to wild-type CHC, monomeric CHC enhances p53-mediated transcription through the recruitment of histone acetyltransferase p300. Immunofluorescent microscopic analysis exhibited that CHC833-1406 is predominantly localized in nuclei, suggesting that there may be a certain regulatory domain for nuclear export in the C-terminus of CHC. Thus, the trimerization domain of CHC is not necessary for the transactivation of p53 target genes and these data provide further evidence that nuclear CHC plays a role distinct from clathrin-mediated endocytosis.
Oncogene advance online publication, 22 October 2007; doi:10.1038/sj.onc.1210854

Keywords: clathrin heavy chain; gene transcription; monomer; p53; tumor suppressor

Introduction

The p53 gene, in which most frequent mutations have been found in human cancers, encodes a protein that plays an important role in preventing tumorigenesis (Levine, 1997; Prives and Hall, 1999; Vogelstein *et al.*, 2000; Vousden and Lu, 2002; Bourdon *et al.*, 2003; Oren, 2003). Although it has been proposed that p53 has various functions such as transcriptional activation for cell cycle arrest and apoptosis (Bourdon *et al.*, 2003; Oren, 2003), centrosome duplication (Tarapore and Fukasawa, 2002), homologous recombination (Linke *et al.*, 2003), nucleotide excision repair (Seo *et al.*, 2002) and transcription-independent mitochondria-mediated apoptosis (Mihara *et al.*, 2003), transcriptional regulation by p53 is thought to be most important for the prevention of tumorigenesis because most p53 mutations in tumor cells are located in the central DNA-binding domain (Hollstein *et al.*, 1991).

The expression level of p53 protein is tightly regulated by various E3 ubiquitin ligases including Mdm2 oncoprotein (Haupt *et al.*, 1997; Honda *et al.*, 1997; Kubbutat *et al.*, 1997), Pirh2 (Leng *et al.*, 2003), COP1 (Dornan *et al.*, 2004) and ARF-BP1/Mule (Chen *et al.*, 2005; Zhong *et al.*, 2005), which bind p53 to degrade it (Brooks and Gu, 2006). In response to various genotoxic stresses such as γ-irradiation, UV and antitumor drugs, p53 is stabilized and activated through post-translational modification including phosphorylation, acetylation and methylation to promote the transcription of various genes responsible for DNA repair (p53R2 and GADD45), growth arrest ($p21^{waf1}$) and apoptosis (Bax, Noxa, Puma and p53AIP1) (Levine, 1997; Prives and Hall, 1999; Vousden and Lu, 2002; Bourdon *et al.*, 2003). Analysis of p53-mediated transcriptional mechanisms is important for the elucidation of tumorigenesis and the development of new antitumor drugs. Although many factors that contribute to the regulation of p53 activity have been reported (Prives and Hall, 1999; Ljungman, 2000; Samuels-Lev *et al.*, 2001), the detailed mechanisms remain to be elucidated. We have recently reported that a serine-to-phenylalanine substitution of p53 at codon 46 (p53S46F) strongly increased the function of p53, leading to the stabilization of the interaction with clathrin heavy chain (CHC) to enhance p53-mediated transcription (Enari *et al.*, 2006). In addition, it has recently been reported that adenovirus-mediated gene transfer of p53S46F suppresses the tumor growth of cancer cells more effectively than that of wild-type p53 *in vivo* (Nakamura *et al.*, 2006).

In the clathrin-mediated endocytic pathway, clathrin is composed of a trimer of CHC and is associated with each

Correspondence: Dr M Enari, Radiobiology Division, National Cancer Center Research Institute, 5-1-1 Tsukiji, Chuo-ku, Tokyo 104-0045, Japan.
E-mail: menari@gan2.res.ncc.go.jp or
Dr Y Taya, SORST, Japan Science and Technology Agency (JST), 5-1-1 Tsukiji, Chuo-ku, Tokyo 104-0045, Japan.
E-mail: ytaya@gan2.res.ncc.go.jp
Received 10 May 2007; revised 15 August 2007; accepted 17 September 2007

light chain, called triskelion, and they further assemble to form a polyhedral cage-like structure (Kirchhausen, 2000). Polyhedral clathrin is recruited to the plasma membrane and promotes the internalization of certain receptors to take nutrients or to transduce correct intracellular signaling from receptors (McPherson *et al.*, 2001). In addition, more recently, it has been reported that CHC plays a role in mitosis (Royle *et al.*, 2005). CHC consists of an N-terminal β-propeller domain that is necessary for binding to adapter proteins for the internalization of various molecules, followed by seven α-helical repeat structures named 'clathrin repeats' (Kirchhausen, 2000). In the C-terminus, CHC possesses a trimerization domain essential for stable formation of the polyhedral clathrin structure (Wakeham *et al.*, 2003). We recently showed that CHC was present in nuclei and that nuclear CHC formed a complex with both p53 and histone acetyltransferase p300 in response to DNA damage. Thus, we demonstrated that CHC has a novel function as a regulator of p53-mediated transcription in addition to the functions for endocytosis and mitosis (Enari *et al.*, 2006). However, it remains elusive whether the trimerized formation of CHC, which is necessary for lattice formation to promote clathrin-dependent endocytosis, is required for p53 transactivation.

In this study, we determined the detailed p53-binding domain of CHC using various deletion mutants of CHC and revealed that CHC bearing residues from 833 to 1406 (CHC833-1406) lacking trimerization and clathrin light chain (CLC)-binding domains interacts with p53. Although CHC833-1406 does not oligomerize, it still has the ability to transactivate p53, indicating that the oligomerization of CHC, which is critical for endocytosis and mitosis, is not necessary for p53-mediated transcription. In addition to our previous observation (Enari *et al.*, 2006), these results further support that CHC has an alternative function as a coactivator for p53 and a different role from the regulation of endocytosis and mitosis.

Results

Trimerization domain of CHC is not required for interaction with p53 and the CLC-binding domain of CHC inhibits interaction with p53

CHC comprises the N-terminal globular domain, which is required for binding to various endocytic adapter proteins to regulate endocytic actions, seven repeat structures designated as clathrin repeats in the middle and C-terminal parts, followed by CLC-binding and trimerization domains in the C-terminus. We have previously determined the interaction domain between CHC and p53 and shown that p53 binds to CHC through the C-terminus of CHC (Enari *et al.*, 2006); however, although the C-terminus of CHC is a major site for p53 binding, the other region of CHC is also required for full binding activity to p53 (data not shown). In order to determine the detailed region that binds to p53, PCR was used to engineer various C-terminal deletion mutants of CHC and they were expressed as ^{35}S-labeled proteins by an *in vitro* transcription/translation system using rabbit reticulocyte lysates (Figure 1a). ^{35}S-labeled CHC proteins were detected as expected bands by autoradiography (Figure 1b) and tested for binding to wild-type p53 fused to glutathione-*S*-transferase (GST-p53wt) in pull-down assays as described previously (Enari *et al.*, 2006). Deletion of residues from 1675 to 1615 (CHC1-1634 and CHC1-1615) does not affect the binding of CHC to p53 (Figure 1b). In contrast, deletion to residues 1522 (CHC1-1522) reduced interaction with p53 (Figure 1b), whereas further deletion of CHC to residues 1406 (CHC1-1406) recovered p53 interaction, suggesting that the C-terminal region containing the trimerization domain on CHC is not necessary for binding to p53 and presumably competes for binding to CLC (Figure 1b).

To assess whether the CLC-binding ability of CHC lacking a trimerization domain increases, two isoforms of CLC proteins were prepared as GST-fusion proteins. The binding affinity of CHC deletion mutants lacking a trimerization domain to both isoforms of GST-CLC proteins is three to fourfold higher than that of wild-type CHC (Figure 1c), consistent with the fact that CHC lacking a trimerization domain has stronger binding activity to CLC than wild-type CHC as assayed using the yeast two-hybrid system (Chen *et al.*, 2002). Thus, these results suggest that the increase of the binding affinity of CHC to CLC leads to the exclusion of p53 from the CHC complex. Mutants with further deletion to residues 1313, 1213 or 1073 had little binding ability to p53, indicating that a major p53-binding site of CHC is located between residues 1313 and 1406 although the N-terminal part of CHC is also required for full binding affinity to p53 (see below).

We next examined the effect of N-terminal deletion of CHC on binding to p53 using GST pull-down assays. As CHC has seven repeat structures (called clathrin repeats) in the middle and C-terminal parts and the predicted tertiary structure of these regions has been reported (Ybe *et al.*, 1999), we constructed various CHC mutants bearing the N-terminal deletion to repeat 1 (aa 686–1675), repeat 2 (aa 833–1675) and repeat 3 (aa 979–1675) to assess which repeat structures are required for binding to p53 (Figure 1d). Analysis of GST pull-down assays revealed that CHC833-1675 had similar p53-binding affinity to wild-type CHC and that further deletion to repeat 3 greatly reduced interaction with p53 (Figure 1e). Furthermore, we generated N- and C-terminal deletions of CHC bearing the region from residues 833 to 1406 (CHC833-1406) and carried out a GST pull-down assay for this deletion mutant (Figure 1f). As expected, CHC833-1406 had full binding affinity to p53 compared to wild-type CHC (Figure 1g). Furthermore, by using the anti-FLAG antibody, we examined the interaction between FLAG-tagged p53 and hemagglutinin(HA)-tagged CHC833-1406 in cells. Immunoblot analysis showed that HA-tagged CHC833-1406 as well as HA-tagged full-length CHC was present in immunoprecipitates containing FLAG-tagged p53 from cell extracts of H1299 cells (Figure 1h), indicating that the region from residues 833 to 1406 on CHC, which corresponds to repeat 3–6, is a minimal p53-binding site for full binding affinity.

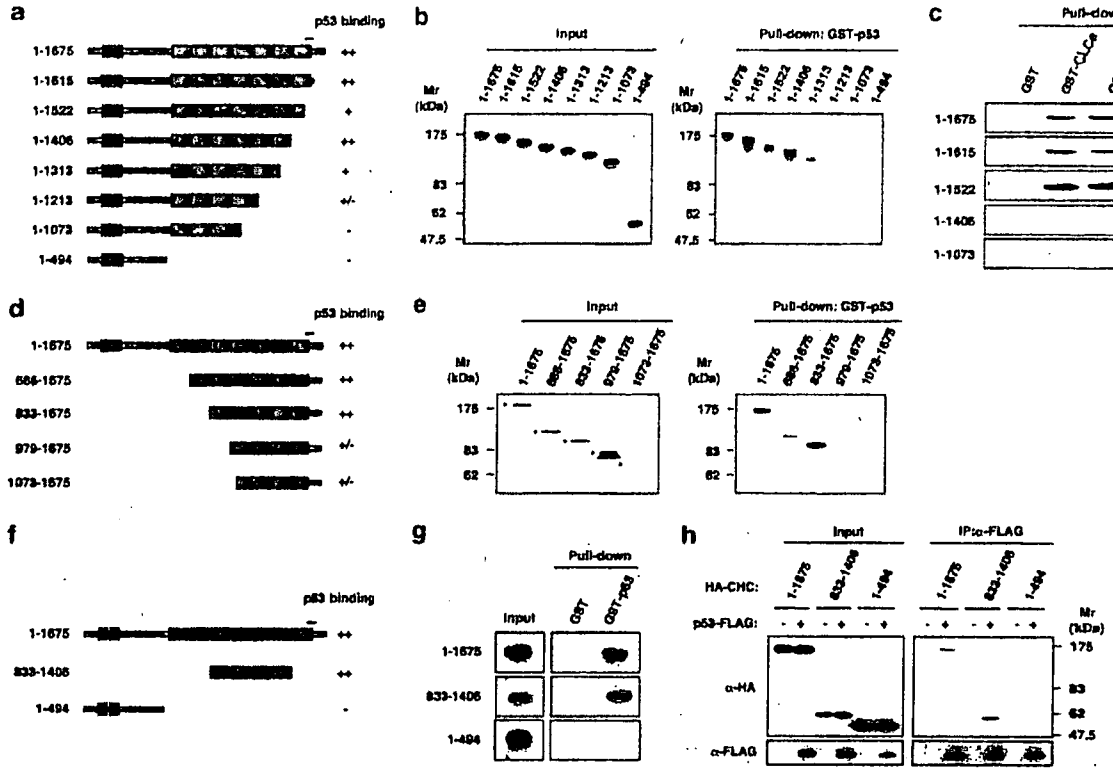

Figure 1 Determination of p53-binding region of clathrin heavy chain (CHC). (a) Schematic representation of full-length CHC (CHC1-1675) and its C-terminal deletion mutants. Blue and red boxes indicate the β-propeller globular domain and clathrin repeat structures, respectively. Trimerization domain is represented by a black bar. (b) Mapping of p53-binding region using CHC mutants with C-terminal truncation. ^{35}S-labeled CHC1-1675 and deletion mutants were synthesized by an in vitro transcription-coupled translation system using rabbit reticulocyte lysates. Lysates containing each ^{35}S-labeled CHC protein were mixed with Sepharose beads immobilized in glutathione-*S*-transferase (GST) or GST fused to wild-type p53 (GST-p53) for binding assays. (c) Mapping of CLC-binding region using N-terminal CHC mutants. Reticulocyte lysates containing each ^{35}S-labeled CHC protein were mixed with Sepharose beads immobilized in GST or GST fused to wild-type CLCa (GST-CLCa) for binding assays. (d) Schematic representation of CHC1-1675 and its N-terminal deletion mutants. (e) Mapping of p53-binding region using N-terminal CHC mutants. ^{35}S-labeled CHC1-1675 and deletion mutants with N-terminal truncation were synthesized and used for *in vitro* binding assays as described in (b). Asterisks indicate various CHC proteins expressed in reticulocyte lysates. (f) Schematic representation of CHC1-1675 and CHC833-1406, which corresponds to clathrin repeat 3 to repeat 6. (g) Requirement of the region between residues 833 and 1406 on CHC for sufficient interaction with p53. ^{35}S-labeled CHC1-1675 and CHC833-1406 were synthesized and used for *in vitro* binding assays. (h) H1299 cells were transfected with each HA-CHC construct in the absence or presence of FLAG-tagged p53 construct. FLAG-tagged p53 in cell lysates was immunoprecipitated by anti-FLAG antibody and eluates were loaded on a 5–20% gradient SDS–polyacrylamide gel, followed by immunoblotting with anti-HA antibody. CHC1-494 was used as a negative control for the immunoprecipitation assay.

CHC binding to p53 correlates with p53 transactivation

When the wild-type CHC construct was cotransfected with p53 expression vector in p53-null H1299 cells, the transactivation of various p53-responsive promoters including p21^{waf1}, Noxa, p53R2 and p53AIP1 promoters, was markedly enhanced compared with those transfected with p53 alone (Enari *et al*., 2006). Under these conditions, we tested the effect of CHC833-1406 on p53 transactivation of various p53-target promoters (p53AIP1, Noxa and p21^{waf1} promoters). Reporter assays using various p53-target promoters showed that the p53-dependent transactivation of all promoters used was enhanced by the expression of CHC833-1406 in both p53-null H1299 and Saos-2 cells (Figures 2a and b), indicating that CHC833-1406 lacking the C-terminal region containing a trimerization domain has similar or rather higher activity to transactivate p53 compared with wild-type CHC. To confirm the effect of CHC833-1406 on its transcriptional activity, the induction of endogenous p53 target genes was monitored by reverse transcriptase-coupled semiquantitative PCR (RT–PCR). RT–PCR experiments showing that the induction of p53-responsive genes was enhanced by the coexpression of CHC833-1406 with p53 up to similar or slightly higher values compared with that by full-length CHC (Figure 2c), although p53 protein level was nearly the same, as judged by immunoblotting (Figure 2d).

The region of CHC from residues 833 to 1406 functions as a monomer

CHC forms a homo-trimer through the trimerization domain located in the C-terminus of CHC and the homo-trimer further assembled to form a cage-like structure

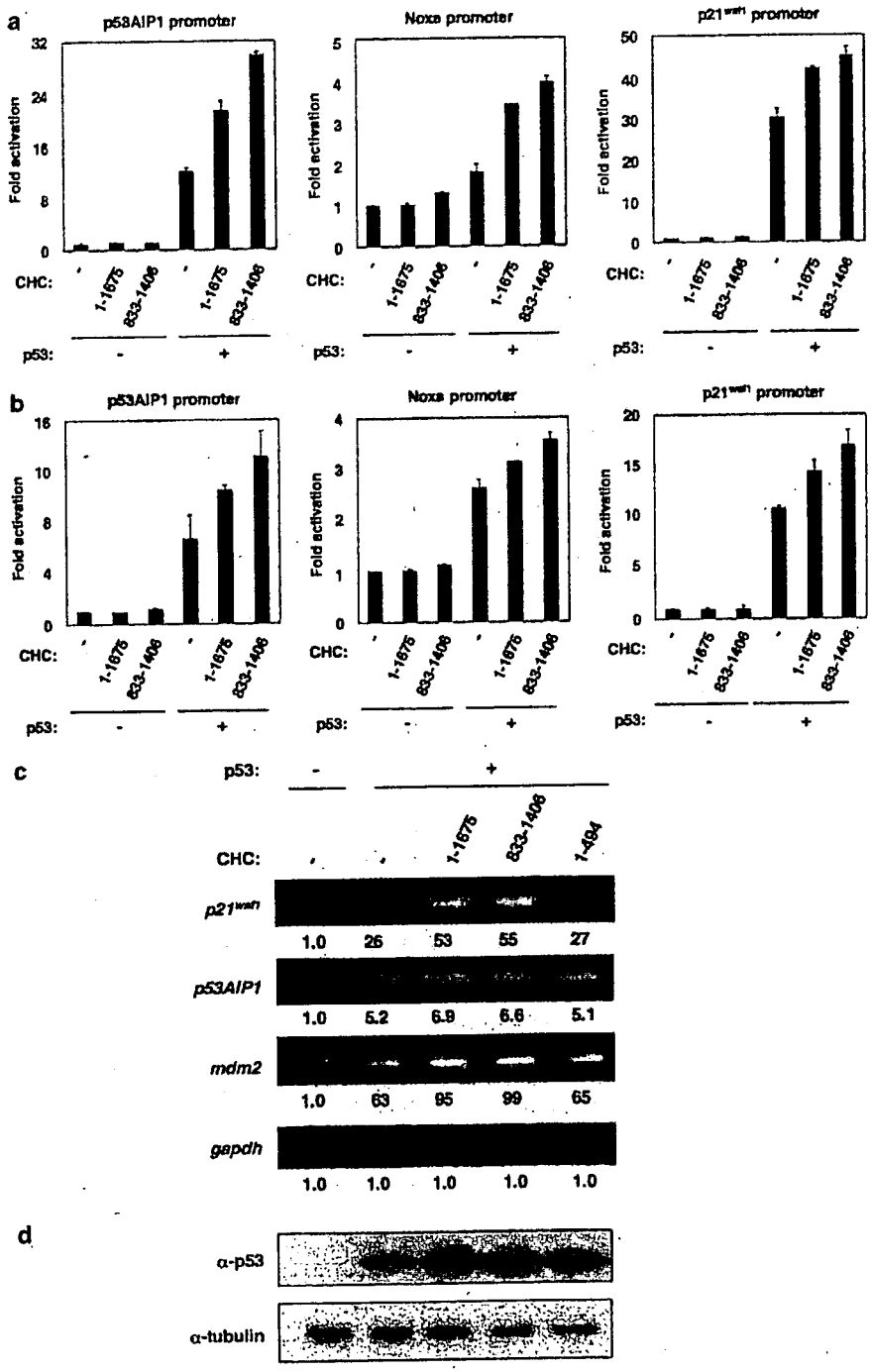

Figure 2 Enhancement of p53-dependent transcription by CHC833-1406. (**a**, **b**) Elevated p53 transactivation by CHC833-1406 using luciferase-based reporter assay. H1299 cells (**a**) and Saos-2 cells (**b**) were transfected with 5 ng of p53 construct, 200 ng of each CHC construct and reporter plasmids as indicated, and luciferase activity was measured at 24 h after transfection. (**c**) Elevation of the expression of endogenous p53-responsive genes by CHC833-1406. H1299 cells were transfected with p53 construct and CHC expression vectors and at 17 h after transfection, expression levels of p53-target genes were analysed by semiquantitative RT–PCR. The intensity of PCR products was quantified by NIH Image software. (**d**) Expression level of p53 in H1299 cells used for RT–PCR experiments. CHC1-494 was used as a negative control for RT–PCR experiments.

responsible for endocytic function; therefore, we assessed whether CHC833-1406 lacking a trimerization domain was indeed present as a monomer under our conditions. To ascertain this, we first carried out an immunoprecipitation assay with various FLAG- and HA-tagged CHC constructs. FLAG- or HA-tagged wild-type CHC or both constructs were transfected into cells and cell lysates were immnoprecipitated with anti-HA antibody. The immune complex was eluted and coprecipitated FLAG-tagged CHC in the eluates was detected by immunoblotting with anti-FLAG antibody. As shown in Figure 3a, FLAG-tagged wild-type CHC was able to associate with HA-tagged wild-type CHC. On the other hand, CHC833-1406 lacking a trimerization domain had no or little ability to associate with any CHC proteins and did not form a homo-oligomer (Figures 3a and b). To further characterize the polymeric status of CHC833-1406, we performed chemical cross-linking experiments, using bis[sulfosuccinimidyl]suberate (BS^3), a bi-functional chemical cross-linker with 11.4 Å arm length, which was chosen because for cross-linking of CHC, dimethyl suberimidate (DMS) with a similar arm length (11.0 Å) has previously been used (Kirchhausen and Harrison, 1981). When recombinant CHC1073-1675 protein purified from *Escherichia coli* was reacted with BS^3 at a concentration of 2 mM, it was cross-linked and the trimerized formation of CHC1073-1675 was detected (Figure 3c). In contrast, CHC833-1406 devoid of a trimerization domain was not oligomerized even when treated with BS^3 and was detected as a monomer, as determined by silver staining (Figure 3c). These data indicate that CHC833-1406, with the ability to transactivate p53, is present as a monomer.

Effect of CHC833-1406 on clathrin-mediated endocytosis

Given that CHC833-1406 did not form an oligomer, we next asked if this CHC mutant could affect clathrin-mediated endocytosis to exclude the possibility that p53 transactivation by CHC is due to the dysfunction of clathrin-dependent endocytosis. Ligand-induced internalization of transferrin receptor occurs via clathrin-mediated endocytosis and the system of transferrin-bound transferrin receptor internalization has been used to analyze clathrin-mediated endocytosis. Using this system, we examined the effect of a monomeric CHC mutant on clathrin-mediated endocytosis. For this experimental procedure, each construct, wild-type CHC or CHC833-1406, was transfected into cells in the absence or presence of the expression vector of short-hairpin RNA (shRNA) against the 3′-untranslated region of CHC mRNA (shRNA-CHCunt) to down-regulate endogenous CHC expression and to see the effect of ectopically expressed CHC on endocytosis. When cells were transfected with wild-type CHC construct without shRNA-CHCunt, the uptake of fluorescent-labeled transferrin slightly increased compared with the control (Figure 4a, Column 1 vs 2), although the amount of cell surface-bound transferrin was almost the same as the control (Figure 4b, Column 1 vs 2). In cells transfected with control vector plus shRNA-CHCunt, the endocytosis of transferrin was severely impaired and decreased by up to 50% (Figure 4a, Column 4), whereas when cells were transfected with wild-type CHC construct plus shRNA-CHCunt, the severe defect of endocytosis by shRNA-CHCunt was recovered up to 90% (Figure 4a, Column 5). Endocytic activity on transferrin uptake well correlates with the expression level of CHC (Figure 4c). Under these conditions, the effect of CHC833-1406 on transferrin endocytosis was similar to that of an empty vector (Figures 4a and b) although the expression of CHC833-1406 and transferrin receptor is similar to that of full-length CHC (Figure 4c), indicating that CHC833-1406 has no or little ability to affect endocytic action.

Monomeric CHC enhances p53-mediated apoptosis

Wild-type CHC enhances p53-mediated apoptosis when cells are cotransfected with CHC and p53 expression vectors or when the CHC construct is transfected into p53-positive cells (Enari *et al*., 2006); therefore, we next addressed whether the monomeric form of CHC has the ability to enhance p53-mediated apoptosis. As caspase activation is a well-characterized marker for apoptosis, caspase-3/7 activation was measured using a fluorogenic substrate. When monomeric CHC833-1406 construct was cotransfected with p53 expression vector, increased caspase-3/7 activity was detected at a higher level than those cotransfected with wild-type CHC and p53 constructs (Figure 5a), although the expression level of p53 between these samples was similar (Figure 5b). Furthermore, we also confirmed this result by monitoring the cleavage of poly-ADP ribose polymerase-1 (PARP-1), which is known as a death substrate (Figure 5c), indicating that monomeric CHC still has the ability to promote p53-mediated apoptosis.

p53 transactivation by monomeric CHC mediates p300

We have previously shown that CHC transactivates p53 through the recruitment of histone acetyltransferase p300 (Enari *et al*., 2006). To investigate whether monomeric CHC833-1406 interacts with p300, an immunoprecipitation assay was performed. HA-tagged CHC833-1406 was present in the immunoprecipitates including FLAG-tagged p300 as well as HA-tagged full-length CHC (Figure 6a). To examine whether CHC833-1406 as well as wild-type CHC cooperates with p300 to stimulate p53-mediated transcriptional activity, a reporter assay using p53AIP1 promoter was used as described above. The ectopic expression of wild-type p300 and p53 with wild-type CHC in p53-null cells greatly enhanced p53 transactivation compared to p53 alone (Figure 6b). Similarly with wild-type CHC, CHC833-1406 enhanced p300-mediated p53 transactivation (Figure 6b). Furthermore, p300DN (residues 1514 to 1922), which works as a dominant-negative p300 for p53-mediated transcription, inhibited CHC833-1406-mediated p53 transactivation (Figure 6c), indicating that the enhancement of p300-mediated p53 transactivation by the monomeric form of CHC is almost equivalent to that by wild-type CHC.

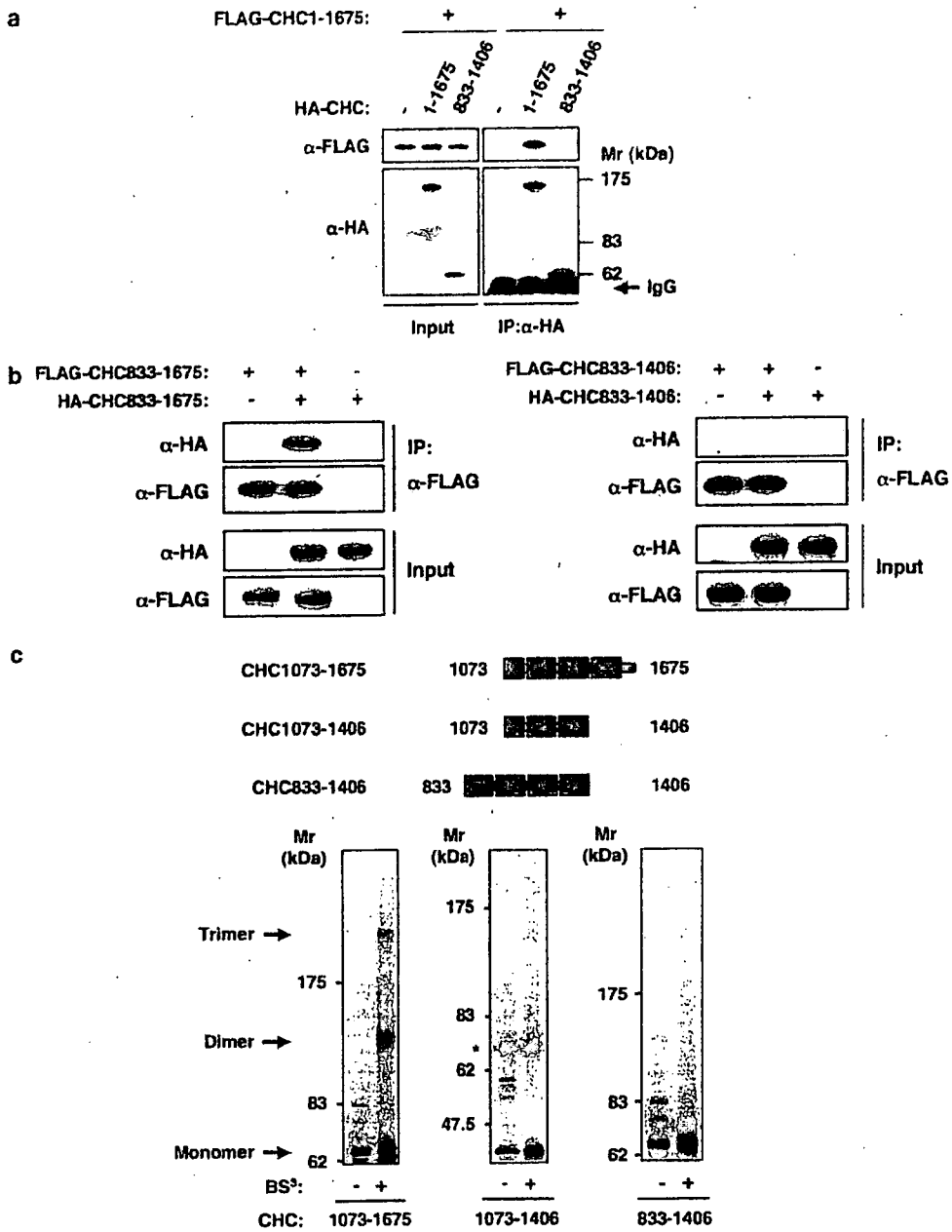

Figure 3 CHC833-1406 is a monomer. (a) CHC833-1406 lacking C-terminal trimerization domain does not interact with full-length CHC1-1675. H1299 cells were transfected with FLAG-tagged full-length CHC1-1675 and HA-tagged full-length CHC1-1675 or CHC833-1406. HA-tagged CHC proteins in cell lysates were immunoprecipitated with anti-HA antibody and immunoblotted with indicated antibodies. (b) CHC833-1406 does not form a homo-oligomer. FLAG-tagged CHC (CHC833-1675 or CHC833-1406) and HA-tagged CHC (CHC833-1675 or CHC833-1406) were ectopically expressed in H1299 cells, and each HA-tagged CHC protein in cell lysates was immunoprecipitated with anti-HA antibody, followed by immunoblotting with indicated antibodies. (c) CHC833-1406 is present as a monomer. Schematic representation of recombinant CHC protein used in crosslinking experiments (Top panel). Silver-staining pattern of crosslinked species from purified CHC proteins (CHC1073-1675, CHC1073-1406 and CHC833-1406) is shown in bottom panels. Recombinant CHC proteins used in this assay were expressed in *E. coli* and purified as described in Materials and methods. Purified CHC proteins were cross-linked with BS^3 at a final concentration of 2 mM for 10 min at 30 °C, and the reaction was stopped by the addition of 1/5 volume of 1 M Tris–HCl (pH 6.8). Cross-linked species were resolved by 10% SDS–polyacrylamide gel electrophoresis and visualized by silver staining. Asterisk indicates a nonspecific band.

Increased nuclear localization of monomeric CHC

We previously showed that approximately 5% of endogenous CHC is present in nuclei and is important for the induction of p53-target genes. To examine the effect of the deletion of the trimerization domain in CHC protein on cellular localization, we performed

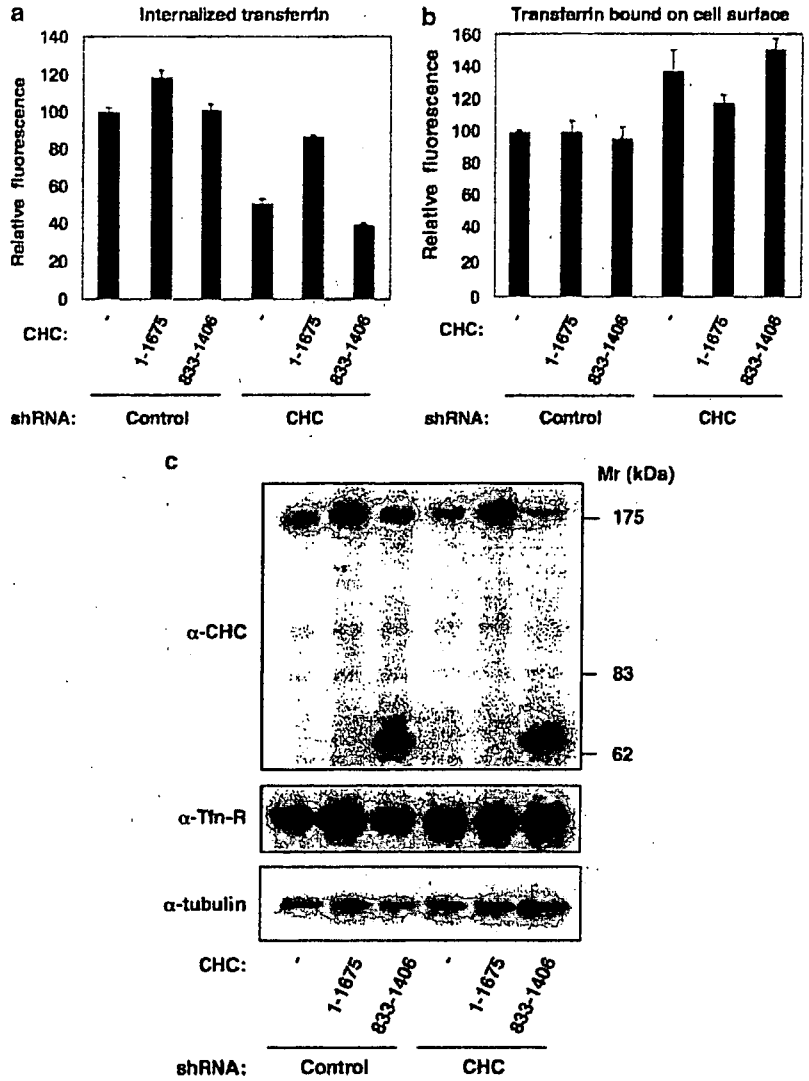

Figure 4 No or little effect of CHC833-1406 expression on clathrin-mediated endocytosis. (a) Expression of CHC833-1406 does not affect transferrin receptor-mediated endocytosis. HeLa cells were transfected with indicated plasmids plus a green fluorescent protein (GFP) expression plasmid. Three days after transfection, cells were incubated for 8 min at 37 °C in DMEM containing 20 μg ml $^{-1}$ of AlexaFluor-594-conjugated transferrin (AF594-transferrin) and 0.1% BSA. After removal of cell surface-bound AF594-transferrin, these cells were trypsinized and fixed with 4% paraformaldehyde. For measurement of AF594-transferrin uptake, GFP-positive cells were quantified by flow cytometric analysis as described in Materials and methods. (b) Analysis of the expression of transferrin receptors on cell surface. HeLa cells were transfected as described in (a), detached with 1 mM EDTA/PBS and incubated on ice for 20 min in DMEM containing 20 μg ml $^{-1}$ of AF594-transferrin and 0.1% BSA. After washing with ice-cold PBS, these cells were fixed and the amount of AF594-transferrin bound on cell surface was quantified by flow cytometric analysis. (c) Expression levels of CHC and transferrin receptor in HeLa cells transfected with pSUPER-CHC and CHC expression vectors. Expression levels of CHC and transferrin receptor in cell lysates from cells transfected as described in (a) were analysed by immunoblotting with anti-CHC (X.22) or antitransferrin receptor antibody for confirmation. The amount of β-tubulin is indicated as a loading control.

confocal immunofluorescent microscopic analysis. HA-tagged wild-type CHC and CHC833-1675 bearing a trimerization domain were mainly localized in cytoplasm and exhibited a similar localization pattern to endogenous CHC (Figures 7a and b and data not shown). However, HA-tagged CHC833-1406 lacking a trimerization domain predominantly accumulated in nuclei and exhibited increased nuclear localization (Figures 7a and b), suggesting that the C-terminal region containing the trimerization domain of CHC is crucial to keep CHC in the cytoplasm. CHC833-1406 may induce p53-mediated apoptosis more efficiently than full-length CHC (Figure 5) due to elevated nuclear accumulation caused by C-terminal deletion of CHC.

Leptomycin B is an inhibitor of nuclear export mediated by CRM1, a nuclear export factor, and blocks the nuclear export of various nucleocytoplasmic shuttle proteins bearing leucine-rich nuclear export signal (NES) sequences (Kumar *et al.*, 2006). To address whether the nuclear accumulation of CHC is dependent

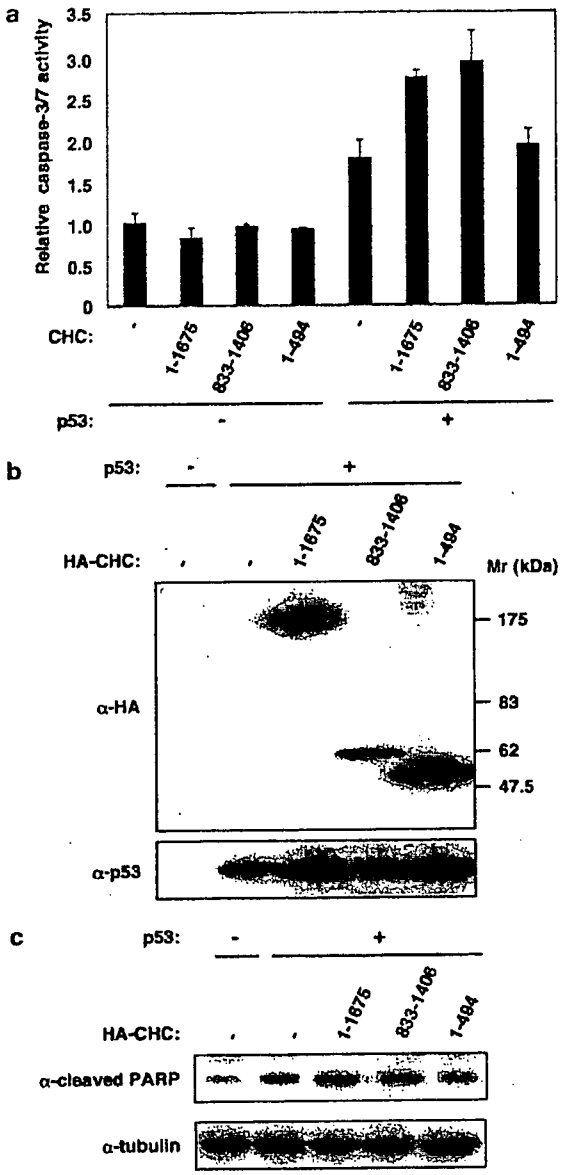

Figure 5 Enhancement of p53-dependent apoptosis by CHC in an oligomerization-independent manner. (a) Enhanced caspase-3/7 activation during apoptosis induced by monomeric CHC in the presence of p53. H1299 cells were transfected with p53 and CHC expression vectors. At 17h after transfection, cells were lysed and caspase-3/7 activity in lysates was determined by fluorometric assay. CHC1-494 was used as a negative control for apoptosis assay. (b) Expression levels of p53 and CHC used for (a). (c) Enhanced PARP-1 cleavage caused by p53-mediated apoptosis in response to monomeric CHC expression. The above samples were immunoblotted with anti-PARP-1 antibody and immunocomplex was detected by enhanced chemiluminescence.

on the classical nuclear export system, we tested the effect of leptomycin B on the nuclear export of CHC. Treatment of cells with leptomycin B induced the nuclear accumulation of p53 fused to NES sequences derived from an inhibitor of cAMP-dependent protein kinase (PKI), which is well known to depend on CRM1 (Figure 7c). In contrast, leptomycin B had no or little effect on the nuclear accumulation of CHC (Figures 7c and d), indicating that the nuclear localization of CHC is mediated by an unidentified nuclear export system and is likely to utilize a distinct nuclear export system from the conventional method.

Discussion

Although CHC was originally identified as a regulator of clathrin-mediated endocytosis, vesicle transport and protein sorting, we have recently demonstrated that a small amount of CHC is present in nuclei and is required for p53-mediated transcription (Enari *et al.*, 2006). Cytosolic CHC is known to be important to trimerize and form a cage-like structure during endocytic action. Moreover, it has recently been reported that the trimerization of CHC is required for mitosis (Royle and Lagnado, 2006); however, it remains elusive whether the trimerization of nuclear CHC is necessary for p53-mediated transcription.

In this study, we generated various CHC deletion mutants and determined the detailed region responsible for interaction with p53. *In vitro* binding analysis using various CHC mutants lacking N- or/and C-terminal regions revealed that the region between residues 833 and 1406 is required for interaction with p53 and that the trimerization domain of CHC is not required for p53 binding (Figure 1). This region corresponds to clathrin repeat 3–6, for which there has been no report regarding binding protein, although part of this region overlapped with CLC binding (Enari *et al.*, 2006). These data are consistent with our previous observation (Enari *et al.*, 2006) that both CLC and p53 bind mutually exclusively to clathrin repeat 6 in this region. Furthermore, the analysis of p53 transactivation using reporter assay indicates that CHC interactions with p53 are required for and correlate with enhanced p53 transactivation (Figure 2).

We recently noted a considerable similarity of the N-terminal transactivation domain of p53 around Ser46 to the CHC-binding region of CLC, and a critical Trp108 residue (bovine CLCa) for CHC binding conserved in p53 (Chen *et al.*, 2002; Enari *et al.*, 2006). Presumably, CLC competes with p53 through this homologous region, in particular through clathrin repeat 6. The tertiary structure of p53-CHC complex remains to be determined and it will give a clue to resolve the mechanisms by which CHC transactivates p53.

It is known that the trimerization domain of CHC is required for endocytic function, and the dysregulation of endocytosis may cause various global alterations including cell survival, cell growth and cell death signalings. To exclude the possibility that p53 transactivation by CHC833-1406 is caused by affecting clathrin-mediated endocytosis, we first performed a coimmunoprecipitation assay. As expected, this assay indicates that neither endogenous CHC nor CHC containing a C-terminal

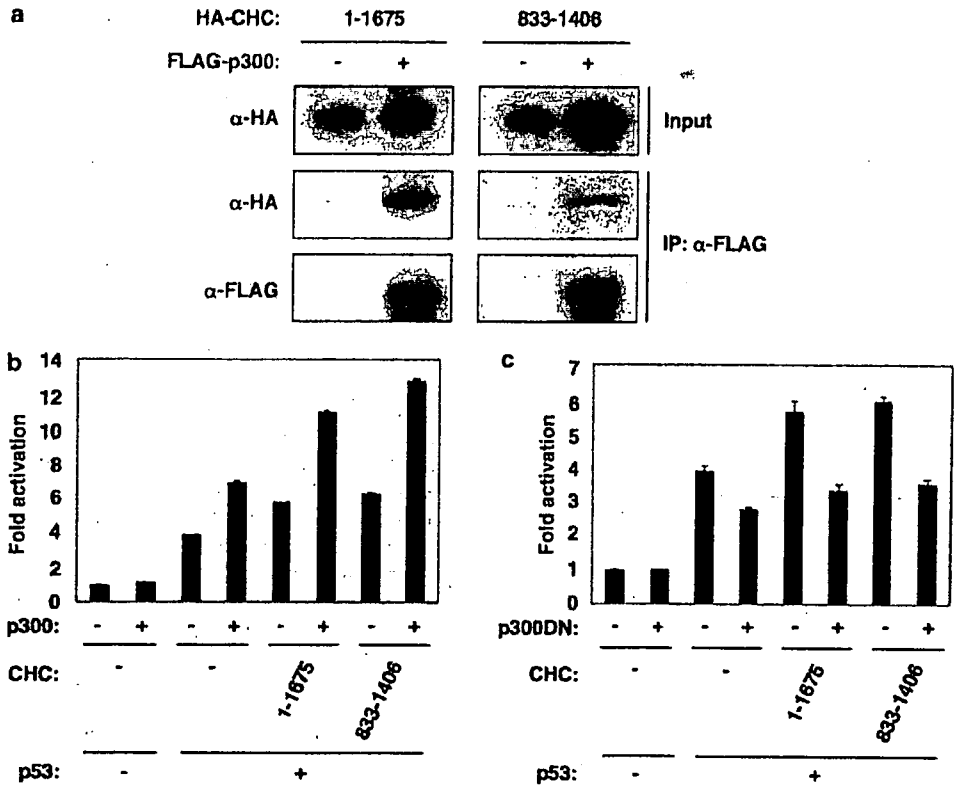

Figure 6 Cooperative effect of CHC and histone acetyltransferase p300 on p53-dependent transcription. (a) p300 interacts with CHC833-1406 as well as full-length CHC1-1675 in cells. H1299 cells were transfected with FLAG-tagged p300 and HA-tagged CHC constructs. Lysates were prepared 48 h after transfection, immunoprecipitated with anti-FLAG antibody and eluates were immunoblotted with indicated antibodies. (b) CHC833-1406 transactivates p53 in collaboration with p300. H1299 cells were transfected with 1 ng of p53 construct, 200 ng of HA-tagged p300 construct, 200 ng of CHC construct and 150 ng of reporter plasmid containing p53AIP1 promoter, and luciferase activity in cell lysates was measured 24 h after transfection. (c) A dominant-negative p300 fragment (p300DN) inhibits CHC833-1406-mediated p53 transactivation. H1299 cells were transfected with 1 ng of p53 construct, 200 ng of FLAG-tagged p300DN construct, 200 ng of CHC construct and 150 ng of reporter plasmid containing p53AIP1 promoter and luciferase activity in cell lysates was measured as described in (b).

trimerization domain was coimmunoprecipitated with FLAG-tagged CHC833-1406 (Figure 3). Furthermore, an assay for the cellular uptake of transferrin supports that CHC833-1406 actually does not affect clathrin-mediated endocytosis (Figure 4). The results demonstrate that CHC833-1406 is present in cells as a monomeric form and has the ability to transactivate p53 in the absence of affecting clathrin-mediated endocytosis (Figure 4). Thus, these findings provide further evidence that CHC plays a distinct role from known CHC functions such as endocytosis and mitosis; however, is monomeric CHC present in cells? Gel filtration and glycerol gradient experiments from various reports suggest that some population of both endogenous and ectopically expressed CHC appears to exist as a monomer in cells, although the authors have not mentioned the polymeric status of CHC (Kim and Kim, 2000; Barth and Holstein, 2004; Royle and Lagnado, 2006). The importance of endogenous monomeric CHC exhibited by hydrodynamic methods remains unclear and further investigation will be required to make sure that monomeric CHC in cells plays an important role in regulating p53-mediated transcription.

Although it has so far been reported that numerous proteins bind to the N-terminal domain of CHC (Kirchhausen, 2000; Dell'Angelica, 2001; Lafer, 2002), there is no report regarding the association with the region identified here as a p53-binding domain corresponding to repeat 3–6. Some endocytic proteins, including β-arrestins, epsin1 and eps15, translocate from cytoplasms to nuclei in response to leptomycin B or physiological cognate ligands for G protein-coupled receptors and have been implicated to function as transcriptional modulators for certain target genes (Vecchi *et al.*, 2001; Kang *et al.*, 2005). As most endocytic regulators bind to CHC at the N-terminal domain that is not required for p53 transactivation, they may not regulate p53-mediated transcription through CHC binding; however, we cannot role out the possibility that certain endocytic regulators may modulate other transcriptional factors in collaboration with nuclear CHC.

CHC is a very abundant protein in cells and most CHC is present in cytoplasm. However, as we have previously reported in recent paper (Enari *et al.*, 2006), approximately 5% of CHC is present in nuclei and required for p53-mediated transcription. Furthermore,

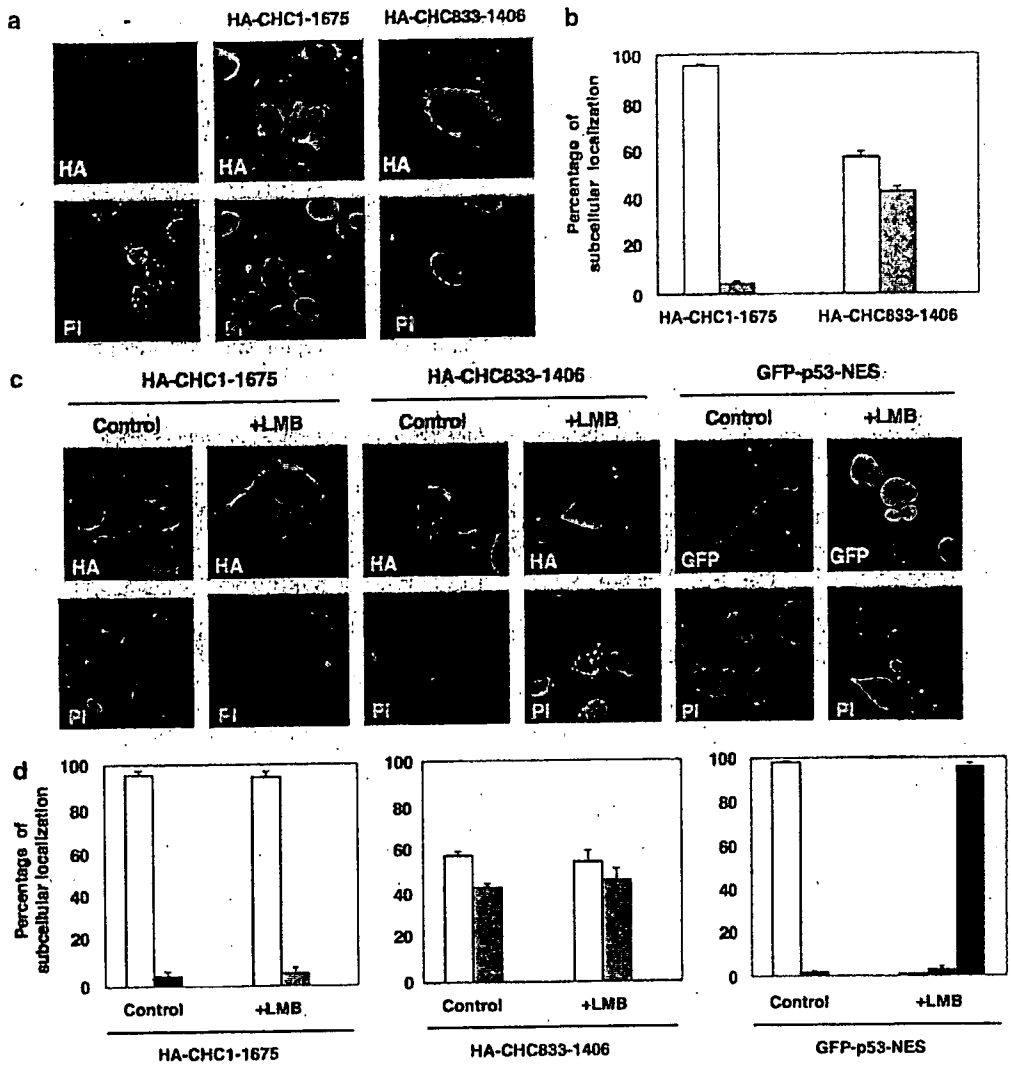

Figure 7 Enhanced nuclear localization of CHC lacking a C-terminal region containing a trimerization domain. (a) Part of CHC833-1406 is localized in nuclei. HA-tagged full-length CHC or CHC833-1406 was expressed in H1299 cells fixed with 4% paraformaldehyde. The fixed cells were sequentially incubated with anti-HA antibody and AlexaFluor-594-conjugated secondary antibody, and subjected to immunofluorescent microscopic analysis. Nuclei were counterstained with propidium iodide (PI). (b) Subcellular localization of CHC in cells was quantified by scoring fluorescent signals from confocal immunofluorescent microscopic analysis. The percentage of cell population of cellular localization was calculated using more than 100 cells in three independent experiments. The percentage of cells, predominantly localized in cytoplasm (open bars), equally localized in cytoplasm and the nucleus (hatched bars), and predominantly localized in the nucleus (black bars) is shown, respectively. (c) Localization of CHC is not affected by treatment with leptomycin B (LMB). H1299 cells were transfected with 400 ng of HA-tagged CHC or 400 ng of GFP-tagged p53 fused to nuclear export signal (NES) construct. The next day, cells were treated with 10 nM LMB for 24 h and analysed by confocal immunofluorescent microscopy. Nuclei were counterstained with PI. (d) Subcellular localization of CHC in cells treated with LMB was quantified by scoring fluorescent signals from immunofluorescent microscopic analysis as described in (b).

immunoelectorn microscopic analysis revealed that CHC is actually present in intact cells, as described previously (Enari *et al*., 2006). To further show this physiological relevance, we quantified how many CHC and p53 molecules are present in nuclei. We purified recombinant CHC and p53 from cells ectopically tansfected with FLAG-tagged CHC or p53 and the concentrations of purified proteins were determined by CBB staining by comparing with known concentrations of bovine serum albumin (BSA). The amounts of CHC and p53 in the cytosolic and nuclear fractions were calculated using the purified CHC and p53. These experiments revealed that 4.74×10^5 molecules of CHC per nucleus is roughly present, on the other hand, 0.34×10^5 molecules of p53 per nucleus is present in DNA-damaged cells, as determined by NIH image Version 1.6.1 densitometry (unpublished data). Thus, nuclear CHC is more abundant than DNA damage-accumulated nuclear p53 even though the

amounts of CHC existing in nuclei is only 5% of total CHC protein, supporting that CHC functions as a coactivator for p53.

Our previous observation that a small fraction of CHC is present in nuclei suggests that a certain part of CHC is required for retention to cytoplasm or the prevention of nuclear import. To explore the mechanism by which the nuclear transport of CHC is regulated, leptomycin B, a specific inhibitor of CRM1/Exportin1-dependent nuclear export, was used in this study. Unfortunately, leptomycin B did not have any effect on the localization of CHC, suggesting that the nuclear transport of CHC is mediated in a CRM1/Exportin1-independent manner (Figure 7). Surprisingly, however, the deletion of the C-terminal region (residues 1523–1675) on CHC leads to elevated nuclear accumulation, suggesting that CHC has the potential to enter the nucleus and that there might be strong nuclear export or cytoplasmic retention sequences in the C-terminal region containing the trimerization domain of CHC. So far, seven nuclear export factors including CRM1, CAS, Exp-t, Exp-4, -5, -6 and -7 have been identified (Kutay and Guttinger, 2005). Also, some transcription factors are retained in the cytoplasm by certain proteins associated with actin and microtubule cytoskeletons (Ziegler and Ghosh, 2005). In future, it will be necessary to elucidate the mechanism for the nuclear transport of CHC to identify which factor is responsible for the cytoplasmic retention of CHC.

In summary, we have defined the minimal p53-binding region of CHC and demonstrated that monomeric CHC still has the ability to transactivate p53. As monomeric CHC has little effect on clathrin-mediated endocytosis and predominantly accumulates in the nucleus to enhance p53-mediated transcription, it can possibly be utilized as an antitumor drug without any side effects.

Materials and methods

Cell culture and transfection

Human lung carcinoma H1299 cells were grown in RPMI 1640 medium supplemented with 10% fetal bovine serum and penicillin/streptomycin. Human cervical carcinoma HeLa cells and human osteosarcoma Saos-2 cells were grown in Dulbecco's modified Eagle's medium (DMEM) supplemented with 10% fetal bovine serum and penicillin/streptomycin at 37°C in a 5% CO_2 atmosphere.

For transfection, cells were plated at 80–90% confluency the day before transfection and transfected with LipofectAmine 2000 reagent (Invitrogen, Carlsbad, CA, USA) according to the manufacturer's protocol.

Plasmids and antibodies

FLAG-tagged p53, HA-tagged and untagged full-length CHC expression plasmids were described previously (Enari *et al.*, 2006). cDNAs encoding each CHC fragment were amplified by PCR and cloned into pcDNA3.1 (Invitrogen) or pCAGGS (Niwa *et al.*, 1991) with and without an HA epitope and confirmed by DNA sequencing. For the expression of shRNA against the 3′-untranslated region of CHC mRNA, synthetic oligoDNAs, 5′-GATCCCCAGAGCACCATGATTCCAATTT CAAGAGATTGGAATCATGGTGCTCTTTTTTGGAAA-3′ and 5′-AGCTTTTCCAAAAAGAGCACCATGATTCCAATT CTCTTGAAATTGGAATCATGGTGCTCTGGG-3′, were annealed and cloned into pSUPER vector (Brummelkamp *et al.*, 2002). Anti-Mdm2 antibody (Ab1) was purchased from Calbiochem. Anti-p21 antibody (SX.118) was purchased from BD Pharmingen (Tokyo, Japan). Horseradish peroxidase-conjugated anti-p53 antibody (DO-1) was purchased from Santa Cruz Biotechnology Inc. (Santa Cruz, CA, USA). Anti-PARP and anti-HA (6E2) antibodies were purchased from Cell Signaling Technology (Beverly, MA, USA). Anti-FLAG antibody (M2) was purchased from Sigma (St Louis, MO, USA). Antitransferrin receptor antibody was purchased from Zymed (San Francisco, CA, USA).

Immunoprecipitation and immunoblotting

H1299 cells (1.8×10^6) were transfected with FLAG-tagged and/or HA-tagged CHC plasmids and harvested at 21 h after transfection. Cells were lysed with lysis buffer (50 mM Tris–HCl at pH 7.2, 250 mM NaCl, 0.1 mM EDTA, 0.1 mM EGTA, 2 mM $MgCl_2$, 0.1% Nonidet P-40, 0.1 mM DTT, 10 μg ml^{-1} antipain, 10 μg ml^{-1} pepstatin, 10 μg ml^{-1} chymostatin, 10 μg ml^{-1} leupeptin, 10 μg ml^{-1} E-64, 10 μg ml^{-1} aPMSF, 1 mM Na_3VO_4 and 10 mM NaF) for 20 min on ice and the lysate was clarified by centrifugation at 20 000 *g* for 20 min. For immunoprecipitation of Flag-tagged protein, the lysate was immunoprecipitated with 10 μl of M2-agarose beads (Sigma) for 2 h and washed three times with lysis buffer. Immunoprecipitates were eluted with 3 × Flag peptide (Sigma) at 4 °C for 30 min, separated by sodium dodecyl sulfate–polyacrylamide gel electrophoresis (SDS–PAGE) and immunoblotted with the indicated antibodies. For immunoprecipitation of HA-tagged proteins, anti-HA antibody (12CA5) and protein G Sepharose (GE Healthcare, Tokyo, Japan) were used. Bound proteins were eluted by boiling at 100 °C for 5 min and subjected to SDS–PAGE, followed by immunoblotting. For immunoblotting, proteins in SDS polyacrylamide gels were transferred to a polyvinylidene fluoride (PDVF) membrane (Millipore, Bedford, MA, USA), the membranes were blocked with 5% nonfat skim milk in tris buffered saline with Tween (TBS-T) buffer (20 mM Tris–HCl at pH 7.6 and 137 mM NaCl and 0.1% Tween 20) for 1 h, sequentially probed with primary antibodies overnight at 4 °C, and a secondary antibody conjugated with horseradish peroxidase for 1 h at room temperature. The antigens were visualized by ECL chemiluminescence (GE Healthcare).

Recombinant proteins and chemical cross-linking

For the expression of various recombinant CHC proteins, cDNAs encoding CHC fragments 1073–1675, 1073–1406 and 833–1406 were cloned into pGEX-6P vector and transformed into *E. coli* DH10B cells. These bacteria harboring each pGEX-CHC plasmid were grown in Luria Broth medium until OD_{600} reached 0.6–0.8. The expression of GST-CHC was induced by the addition of isopropyl-D-thiogalactopyranoside (IPTG) at a final concentration of 0.1 mM and continuous culture at 30 °C for 3 h. Cells were spun and disrupted by sonication at 4 °C and the lysates were centrifuged at 20 000 *g* at 4 °C for 10 min. The resultant supernatants were mixed with glutathione-Sepharose 4B (GE Healthcare) for 1 h at 4 °C. The beads were washed four times with 25 mM Hepes-NaOH at pH 7.5, 150 mM NaCl, 0.1 mM DTT and recombinant CHC proteins were eluted with eight units of PreScission protease (GE Healthcare) at 4 °C overnight.

For chemical cross-linking, each purified CHC fragment was diluted in 25 mM Hepes-NaOH (pH 7.5) 150 mM NaCl to a

concentration of 20 μg ml^{-1}. To provide adequate buffering capacity, 1/5 volume of 1 M triethanolamine at pH 8.5 was added. A chemical cross-linker BS^3 (Pierce Chemical Co., Rockford, IL, USA) was dissolved in 5 mM sodium citrate (pH 5.0) and used for this assay within 2 min. One volume of 10 mM BS^3 was mixed with four volumes of protein samples and incubated at 30 °C for 10 min. The cross-linking reaction (10 μl) was terminated by the addition of 1/5 volume (2 μl) of 1 M Tris–HCl at pH 6.8. Samples were boiled for 2 min, separated by SDS–PAGE and visualized by silver staining.

Endocytosis assay

To analyze the effect of CHC fragments on endocytic activity, HeLa cells (3×10^5) were transfected with 1 μg of pSUPER-CHC plus 2 μg of pCAGGS-CHC vectors in combination with 50 ng of pmaxGFP vector (Amaxa), a transfection marker. Three days after transfection, cells were incubated in DMEM containing 0.1% BSA for 3 h, followed by treatment with 20 μg ml^{-1} Alexafluor-594-conjugated transferrin (AF594-transferrin, Molecular Probes) for 8 min at 37 °C. Cells were rapidly chilled by extensive washing with ice-cold phosphate-buffered saline (PBS) and then AF594-transferrin bound on the cell surface was removed by washing with ice-cold acid-washing buffer containing 0.2 M acetic acid (pH 4.5) and 0.5 M NaCl. These cells were trypsinized, fixed with 4% paraformaldehyde in PBS for 20 min at room temperature and resuspended in 0.1% BSA in PBS. Relative fluorescence was quantified by flow cytometric analysis (Beckton Dickinson, Franklin, NJ, USA) for internalized AF594-transferrin.

To measure transferrin receptors present on the cell surface, cells were first detached using PBS containing 1 mM EDTA and incubated on ice with 20 μg ml^{-1} AF594-transferrin for 20 min. Cells were then washed once with ice-cold PBS, fixed with 4% paraformaldehyde in PBS for 20 min at room temperature and then resuspended in 0.1% BSA in PBS. Relative fluorescence was quantified by flow cytometric analysis for surface-bound AF594-transferrin.

RT–PCR

RT–PCR assay was performed essentially as described in Enari *et al.* (2006). Briefly, total RNA was isolated using an RNeasy mini kit (QIAGEN, Valencia, CA, USA) and five micrograms of total RNA were reverse-transcribed with Superscript II first-strand synthesis kit (Invitrogen) using an oligo-dT primer. Reverse-transcribed products were used for semiquantitative PCR. Primer sequences and PCR programs were described in Enari *et al.* (2006). PCR products were resolved by 2% agarose gel electrophoresis and visualized by ethidium bromide.

Reporter assay

Reporter assay was performed essentially as described previously (Enari *et al.*, 2006). In brief, H1299 cells (4×10^4) or Saos-2 cells (3×10^4) plated on 24-well plates were transfected with 1–5 ng of pC53-SN3, 200 ng of pcDNA3.1-CHC, 200 ng of pCMVβ-p300 and 150 ng of the indicated reporter vectors in combination with 10 ng of phRG-TK encoding Renilla luciferase as an internal control. At 24 h after transfection, cells were harvested and luciferase activity was quantified by a dual luciferase assay system (Promega, Madison, WI, USA) according to the manufacture's instructions.

Apoptosis assay

For caspase-3/7 assay, H1299 cells (2×10^5) were transfected with 50 ng of pC53-SN3 with or without 2 μg of pcDNA3.1-CHC. After 17 h incubation, cells were harvested and caspase-3/7 activity in the cell lysates was measured by CaspACE assay kit using fluorogenic substrates (Promega) according to the manufacture's instructions.

In vitro *binding assay*

To analyze the interaction between CHC and p53, GST-pull-down assay was carried out as described previously (Enari *et al.*, 2006). In brief, bacterial lysates containing p53 fused to GST (GST-p53) were incubated with glutathione-Sepharose beads (GE Healthcare) and washed extensively with binding buffer (50 mM Tris–HCl at pH7.2, 250 mM NaCl, 0.1 mM EDTA, 0.1 mM EGTA, 2 mM $MgCl_2$, 0.1% Tween 20, 0.1 mM DTT, 10 μg ml^{-1} antipain, 10 μg ml^{-1} pepstatin, 10 μg ml^{-1} chymostatin, 10 μg ml^{-1} leupeptin, 10 μg ml^{-1} E-64, 10 μg ml^{-1} aPMSF, 1 mM Na_3VO_4, 10 mM NaF). ^{35}S-labeled full-length CHC and its deletion derivatives were synthesized using an *in vitro* transcription/translation-coupled reticulocyte lysate system (Promega). Lysates containing ^{35}S-labeled CHC proteins were diluted in 12 volumes of binding buffer and incubated with the above beads immobilized with GST-p53 at 4 °C for 2 h. After washing with 1 ml of binding buffer, bound proteins were eluted by boiling in SDS sample-loading buffer for 5 min, subjected to 10% SDS–PAGE and analysed by autoradiography.

Immunofluorescence

H1299 cells (2×10^4) were plated in an 8-well Labtek II chamber (NalgeNunc, Tokyo, Japan). The next day, cells were transfected with 400 ng of pcDNA3.1-HA-CHC and incubated for 24 h. Cells were fixed with 4% paraformaldehyde in PBS, permeabilized with 0.1% Triton X-100 and blocked with 3% BSA in PBS. The chamber was sequentially incubated with anti-HA antibody for 1 h at room temperature and AlexaFluor488- or AlexaFluor594-labeled secondary antibody (Molecular Probes, Eugene, OR, USA), and mounted with Vectashield (Vector Laboratories, Burlingame, CA, USA). Confocal immunofluorescence was performed using an ECLIPSE E600 fluorescence microscope (Nikon, Tokyo, Japan) equipped with a Radiance 2000 imaging system (Bio-Rad, Hercules, CA, USA). To quantify the subcellular localization of CHC, more than 100 cells per sample were counted.

Acknowledgements

We thank Drs T Nagase and M Ohishi (Kazusa DNA Research Institute) for the full-length CHC clone (K1AA0034), Dr I Kitabayashi (National Cancer Center Research Institute) for FLAG-tagged and HA-tagged p300 constructs, Dr B Vogelstein (Johns Hopkins University) for the WWP-Luc reporter plasmid, Drs H Arakawa and Y Nakamura (The University of Tokyo) for the reporter vector containing p53AIP1 promoter, and Drs T Shibue and T Taniguchi for the reporter vector of Noxa promoter (The University of Tokyo), respectively. This work was supported by MEXT, KAKENHI (17013088) and a Grant-in-Aid from the Ministry of Health, Labor and Welfare for the 3rd Term Comprehensive 10-year Strategy for Cancer Control (to YT).

References

Barth M, Holstein SE. (2004). Identification and functional characterization of Arabidopsis AP180, a binding partner of plant alphaC-adaptin. *J Cell Sci* **117**: 2051–2062.

Bourdon JC, Laurenzi VD, Melino G, Lane D. (2003). p53: 25 years of research and more questions to answer. *Cell Death Differ* **10**: 397–399.

Brooks CL, Gu W. (2006). p53 ubiquitination: Mdm2 and beyond. *Mol Cell* **21**: 307–315.
Brummelkamp TR, Bernards R, Agami R. (2002). A system for stable expression of short interfering RNAs in mammalian cells. *Science* **296**: 550–553.
Chen CY, Reese ML, Hwang PK, Ota N, Agard D, Brodsky FM. (2002). Clathrin light and heavy chain interface: alpha-helix binding superhelix loops via critical tryptophans. *EMBO J* **21**: 6072–6082.
Chen D, Kon N, Li M, Zhang W, Qin J, Gu W. (2005). ARF-BP1/mule is a critical mediator of the ARF tumor suppressor. *Cell* **121**: 1071–1083.
Dell'Angelica EC. (2001). Clathrin-binding proteins: got a motif? Join the network!. *Trends Cell Biol* **11**: 315–318.
Dornan D, Wertz I, Shimizu H, Arnott D, Frantz GD, Dowd P *et al*. (2004). The ubiquitin ligase COP1 is a critical negative regulator of p53. *Nature* **429**: 86–92.
Enari M, Ohmori K, Kitabayashi I, Taya Y. (2006). Requirement of clathrin heavy chain for p53-mediated transcription. *Genes Dev* **20**: 1087–1099.
Haupt Y, Maya R, Kazaz A, Oren M. (1997). Mdm2 promotes the rapid degradation of p53. *Nature* **387**: 296–299.
Hollstein M, Sidransky D, Vogelstein B, Harris CC. (1991). p53 mutations in human cancers. *Science* **253**: 49–53.
Honda R, Tanaka H, Yasuda H. (1997). Oncoprotein MDM2 is a ubiquitin ligase E3 for tumor suppressor p53. *FEBS Lett* **420**: 25–27.
Kang J, Shi Y, Xiang B, Qu B, Su W, Zhu M *et al*. (2005). A nuclear function of beta-arrestin1 in GPCR signaling: regulation of histone acetylation and gene transcription. *Cell* **123**: 833–847.
Kim HL, Kim JA. (2000). Purification of clathrin assembly protein from rat liver. *Exp Mol Med* **32**: 222–226.
Kirchhausen T. (2000). Clathrin. *Annu Rev Biochem* **69**: 699–727.
Kirchhausen T, Harrison SC. (1981). Protein organization in clathrin trimers. *Cell* **23**: 755–761.
Kubbutat MH, Jones SN, Vousden KH. (1997). Regulation of p53 stability by Mdm2. *Nature* **387**: 299–303.
Kumar S, Saradhi M, Chaturvedi NK, Tyagi RK. (2006). Intracellular localization and nucleocytoplasmic trafficking of steroid receptors: an overview. *Mol Cell Endocrinol* **246**: 147–156.
Kutay U, Guttinger S. (2005). Leucine-rich nuclear-export signals: born to be weak. *Trends Cell Biol* **15**: 121–124.
Lafer EM. (2002). Clathrin-protein interactions. *Traffic* **3**: 513–520.
Leng RP, Lin Y, Ma W, Wu H, Lemmers B, Chung S *et al*. (2003). Pirh2, a p53-induced ubiquitin-protein ligase, promotes p53 degradation. *Cell* **112**: 779–791.
Levine AJ. (1997). p53, the cellular gatekeeper for growth and division. *Cell* **88**: 323–331.
Linke SP, Sengupta S, Khabie N, Jeffries BA, Buchhop S, Miska S *et al*. (2003). p53 interacts with hRAD51 and hRAD54, and directly modulates homologous recombination. *Cancer Res* **63**: 2596–2605.
Ljungman M. (2000). Dial 9-1-1 for p53: mechanisms of p53 activation by cellular stress. *Neoplasia* **2**: 208–225.
McPherson PS, Kay BK, Hussain NK. (2001). Signaling on the endocytic pathway. *Traffic* **2**: 375–384.
Mihara M, Erster S, Zaika A, Petrenko O, Chittenden T, Pancoska P *et al*. (2003). p53 has a direct apoptogenic role at the mitochondria. *Mol Cell* **11**: 577–590.
Nakamura Y, Futamura M, Kamino H, Yoshida K, Nakamura Y, Arakawa H. (2006). Identification of p53-46F as a super p53 with an enhanced ability to induce p53-dependent apoptosis. *Cancer Sci* **97**: 633–641.
Niwa H, Yamamura K, Miyazaki J. (1991). Efficient selection for high-expression transfectants with a novel eukaryotic vector. *Gene* **108**: 193–199.
Oren M. (2003). Decision making by p53: life, death and cancer. *Cell Death Differ* **10**: 431–442.
Prives C, Hall PA. (1999). The p53 pathway. *J Pathol* **187**: 112–126.
Royle SJ, Bright NA, Lagnado L. (2005). Clathrin is required for the function of the mitotic spindle. *Nature* **434**: 1152–1157.
Royle SJ, Lagnado L. (2006). Trimerisation is important for the function of clathrin at the mitotic spindle. *J Cell Sci* **119**: 4071–4078.
Samuels-Lev Y, O'Connor DJ, Bergamaschi D, Trigiante G, Hsieh JK, Zhong S *et al*. (2001). ASPP proteins specifically stimulate the apoptotic function of p53. *Mol Cell* **8**: 781–794.
Seo YR, Fishel ML, Amundson S, Kelley MR, Smith ML. (2002). Implication of p53 in base excision DNA repair: *in vivo* evidence. *Oncogene* **21**: 731–737.
Tarapore P, Fukasawa K. (2002). Loss of p53 and centrosome hyperamplification. *Oncogene* **21**: 6234–6240.
Vecchi M, Polo S, Poupon V, van de Loo JW, Benmerah A, Di Fiore PP. (2001). Nucleocytoplasmic shuttling of endocytic proteins. *J Cell Biol* **153**: 1511–1517.
Vogelstein B, Lane D, Levine AJ. (2000). Surfing the p53 network. *Nature* **408**: 307–310.
Vousden KH, Lu X. (2002). Live or let die: the cell's response to p53. *Nat Rev Cancer* **2**: 594–604.
Wakeham DE, Chen CY, Greene B, Hwang PK, Brodsky FM. (2003). Clathrin self-assembly involves coordinated weak interactions favorable for cellular regulation. *EMBO J* **22**: 4980–4990.
Ybe JA, Brodsky FM, Hofmann K, Lin K, Liu SH, Chen L *et al*. (1999). Clathrin self-assembly is mediated by a tandemly repeated superhelix. *Nature* **399**: 371–375.
Zhong Q, Gao W, Du F, Wang X. (2005). Mule/ARF-BP1, a BH3-only E3 ubiquitin ligase, catalyzes the polyubiquitination of Mcl-1 and regulates apoptosis. *Cell* **121**: 1085–1095.
Ziegler EC, Ghosh S. (2005). Regulating inducible transcription through controlled localization. *Sci STKE* **2005**: re6.

Regulation of clathrin-mediated endocytosis by p53

Yoshie Endo[1,2,3], Atsumi Sugiyama[1,2], Shun-Ai Li[4], Kazuji Ohmori[1,2], Hirokazu Ohata[1,2], Yusuke Yoshida[1,2], Masabumi Shibuya[3], Kohji Takei[4], Masato Enari[1,2,*] and Yoichi Taya[1,2,*]

[1]*Radiobiology Division, National Cancer Center Research Institute, Tokyo, Japan*
[2]*SORST, Japan Science and Technology Agency (JST), 5-1-1 Tsukiji, Chuo-ku, Tokyo 104-0045, Japan*
[3]*Division of Genetics, Institute of Medical Science, University of Tokyo, 4-6-1 Shirokane-dai, Minato-ku, Tokyo 108-8639, Japan*
[4]*Department of Neuroscience, Okayama University, Graduate School of Medicine and Dentistry, 2-5-1 Shikata-cho, Okayama 700-8558, Japan*

The p53 gene encodes a multi-functional protein to prevent tumorigenesis. Although there have been many reports of the nuclear functions of p53, little is known about the cytosolic functions of p53. Here, we found that p53 is present in cytosol as well as nuclei under unstressed conditions and binds to clathrin heavy chain (CHC). CHC is known to play a role in receptor-mediated endocytosis. Based on our findings, we examined the effect of p53 on clathrin-mediated endocytosis of epidermal growth factor receptor (EGFR). Surprisingly, p53 co-localized with CHC at the plasma membrane in response to EGF stimulation. In cells with ablated p53 expression by RNAi, EGFR internalization was delayed and intracellular signaling from EGFR was altered. Thus, our findings provide evidence that cytosolic p53 may participate in the regulation of clathrin-mediated endocytosis to control the correct signaling from EGFR.

Introduction

The uptake of various substances including nutrients, peptide hormones and extracellular macromolecules into cells is mainly regulated by receptor-mediated endocytosis (Stahl & Schwartz 1986; Mukherjee *et al.* 1997). It has previously been proposed that receptor-mediated endocytosis is required for not only the uptake of nutrients but also the down-regulation of growth factor receptors by sorting into lysosomal compartment to degrade them and to attenuate intracellular signaling from their receptors (Vieira *et al.* 1996). In addition, several lines of evidence suggest that receptor-mediated endocytosis plays an important role in the regulation of spatial and temporal coordination to transduce the downstream signaling from receptors have gradually increased (Di Fiore & Gill 1999; Wiley & Burke 2001; Sorkin & Von Zastrow 2002; Polo & Di Fiore 2006). Most growth factors control diverse intracellular signaling via activation of their specific receptor tyrosine kinases (RTKs) (Alroy & Yarden 1997). Constitutive activation of RTK-mediated pathways is considered to result in tumorigenesis. So far, it has been reported that the aberrant expression of various endocytic proteins, which includes over-expression, deletion, translocation and mutation, was found in various human cancers (Floyd & De Camilli 1998). Although the relationship between endocytic regulation and tumorigenesis has been implicated (Floyd & De Camilli 1998), the mechanism by which the dysregulaion of endocytosis links to tumorigenesis is poorly understood.

One of the most characterized receptors to study the mechanisms of clathrin-mediated endocytosis of receptors is a system of epidermal growth factor (EGF)-induced internalization of EGF receptor (EGFR). EGF triggers the recruitment of various adaptor proteins to EGFR through post-translational modifications such as phosphorylation and ubiquitination (Levkowitz *et al.* 1998; Citri & Yarden 2006). Activated EGFR is internalized and degraded by endocytic regulators including AP2, CHC, Grb2, dynamin-2, Cbl, Eps15, Epsins, STAM, Hrs, TSG101 and ESCRT to terminate signals from EGFR (Sebastian *et al.* 2006). It has been proposed that the route of internalized receptors is individually distinguished even though their internalization is mediated by clathrin. Ligand-induced internalized receptors including EGFR and LDLR travel to early endosome along with microtubules, whereas internalized transferrin receptor (TfnR)

Communicated by: Yoshihiro Nakatani
**Correspondence*: Emails: ytaya@gan2.res.ncc.go.jp; menari@gan2.res.ncc.go.jp

DOI: 10.1111/j.1365-2443.2008.01172.x

migrates slower in a microtubule-independent manner (Lakadamyali *et al.* 2006). Although many proteins including clathrin-coated vesicles have so far been identified by proteomic analyses (Blondeau *et al.* 2004; Borner *et al.* 2006), studies have been unsuccessful in identifying regulators contributing to the early events of EGFR internilization because of the difficulty of isolating clathrin-coated pits.

The tumor-suppressor protein p53, which is encoded by the most frequently mutated gene in human cancers, mainly functions in the nucleus as a transcription factor that activates the transcription of various target genes including DNA repair, cell cycle arrest, apoptosis and anti-angiogenesis (Levine 1997; Prives & Hall 1999; Vousden & Lu 2002; Bourdon *et al.* 2003; Oren 2003). However, several reports from other groups have demonstrated that p53 is present not only in the nucleus to promote the transcription of anti-tumor-responsive genes but also in cytosol, mitochondria and centrosomes to prevent tumorigenesis through other mechanisms (Moll & Zaika 2001; Tarapore & Fukasawa 2002). It has been shown that p53 directly binds to the mitochondrial outer membrane and induces mitochondria-mediated apoptosis (Dumont *et al.* 2003; Mihara *et al.* 2003; Chipuk *et al.* 2004). On the other hand, p53 is also targeted to centrosomes for the prevention of aberrant centrosome duplication during cell cycle progression (Tarapore & Fukasawa 2002; Shinmura *et al.* 2006). While there have been huge numbers of reports regarding p53 functions in the nucleus, the functions of cytosolic p53, in particular at the plasma membrane, remain to be analyzed.

In recent studies, we have shown that p53 interacts with clathrin heavy chain (CHC) in the nucleus, and nuclear CHC is required for p53-mediated transcription (Enari *et al.* 2006). As CHC was originally identified as a cytosolic protein that regulates clathrin-mediated endocytosis, it is assumed that p53 could bind to CHC in cytosol and might regulate clathrin-mediated endocytosis through the association with CHC.

In this paper, we show that p53 associates with CHC not only in nuclei but also in cytosol, and co-localizes with CHC at the plasma membrane in normal human fibroblast and human cancer cells. Surprisingly, p53 also co-localizes with EGF and CHC at the plasma membrane in response to EGF treatment. Moreover, co-immunopurification assay revealed that p53 is contained in the EGFR complex including endocytic regulators. In addition, the ablation of p53 expression by RNA interference (RNAi) causes the delayed uptake of EGF and transduces the aberrant signaling from EGFR, suggesting that p53 regulates the endocytosis of EGFR to transduce accurate signaling from its receptor.

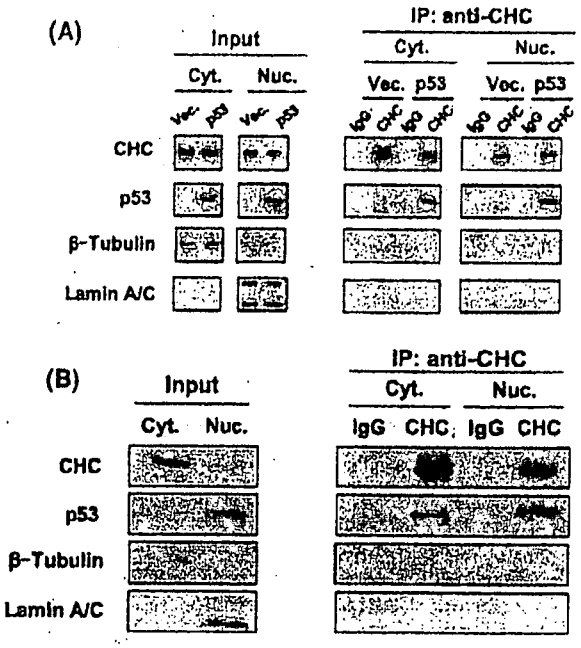

Figure 1 p53 is present in the cytoplasm and associates with CHC in cytosol. (A) Cytosolic (Cyt.) and nuclear (Nuc.) fractions were extracted from p53-null H1299 cells transfected with empty vector or FLAG-tagged p53 construct. Each extract (300 μg) was immunoprecipitated with mouse IgG or anti-CHC antibody and immunoblotted with the indicated antibodies. Input (5%) was shown in the left panel. (B) Cytosolic (Cyt.) and nuclear (Nuc.) fractions were extracted from TIG-7 cells grown under normal culture conditions. Fractions (100 μg) were immunoprecipitated with mouse IgG or anti-CHC antibody, followed by immunoblotting with the indicated antibodies. Anti-β-tubulin and anti-lamin A/C antibodies were used as markers for the purity of each fraction, respectively.

Results

p53 interacts with CHC in cytosol

We have recently shown that CHC is also present in nuclei and interacts with p53 to promote p53-mediated transcription (Enari *et al.* 2006). Based on our knowledge that nuclear CHC binds to p53, we tested whether CHC could also interact with p53 in cytosol. For co-immunoprecipitation experiments, either wild-type p53 construct or empty vector was transfected into p53-null H1299 cells, and cytosolic and nuclear fractions from transfected cells were prepared by homogenization with a Dounce homogenizer. Both fractions were immunoprecipitated with control IgG or anti-CHC antibody, followed by immunoblotting with anti-p53 antibody. As shown in Fig. 1A, p53 was present in cytosolic fractions

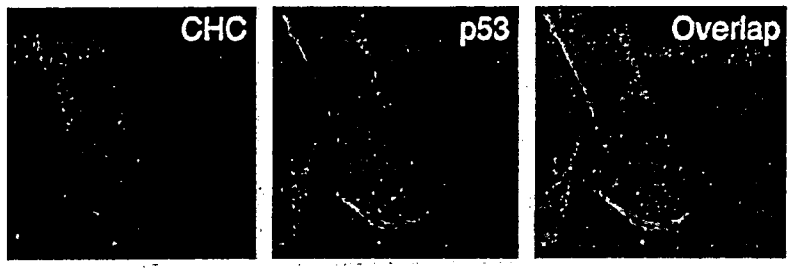

Figure 2 p53 co-localized with CHC at the plasma membrane. TIG-7 cells were processed for double immunofluorescence labeling with antibodies against CHC (TD.1; red: AF594 staining) or p53 (FL393; green: AF488 staining). Staining was analyzed by confocal microscopy. Inset: Higher magnification images of white rectangles. In inset overlap, co-localization of p53 and CHC at the plasma membrane is visible as yellow staining.

and co-immunoprecipitated with cytosolic CHC as well as nuclear CHC. We also examined whether a physical interaction could be detected using normal human fibroblast TIG-7 cells expressing endogenous wild-type p53 (Fig. 1B). Immunoprecipitation analysis showed that p53 was present in immunoprecipitates containing CHC. In addition, when cytosolic and nuclear extracts from p53-positive A549 and MCF-7 cells were immunoprecipitated with anti-CHC antibody, p53-CHC interaction was also detected as efficiently as seen in TIG-7 cells (data not shown), indicating that p53 physically associates with CHC not only in nuclei but also in cytoplasm.

Intracellular localization of p53

We next investigated the subcellular localization of p53 in cells to address whether p53 co-localizes with CHC. For localization of p53, we used normal human fibroblast TIG-7 cells because TIG-7 cells had large and flat cytoplasm, and it is easy to distinguish p53 localization in cytoplasm. Confocal microscopic analysis revealed that a small amount of p53 localizes in cytosol under normal culture conditions though most p53 localizes in nuclei (Fig. 2). Interestingly, some p53 (in 10%–20% of total cells) co-localized with CHC and was present at the plasma membrane, as judged by overlays with a staining pattern of CHC (Fig. 2).

Wild-type p53 but not tumor-derived p53 mutants is recruited to the plasma membrane in response to EGF treatment

Clathrin-mediated endocytosis of EGFR is a well-established system to study endocytic mechanisms; therefore, we next examined whether the localization of p53 is changed by treatment with EGF. Cells were incubated in serum-free medium for 3 h, treated without or with EGF on ice, and indirect immunofluorescent analysis was performed using anti-p53 (FL393) and anti-CHC (TD.1) antibodies. In cells without EGF treatment, most p53 did not exhibit co-localization with CHC at the plasma membrane in serum-starved cells (unlike cells incubated under normal culture conditions), suggesting that the removal of serum containing various growth factors leads to the decreased localization of p53 with CHC at the plasma membrane (Fig. 3A). Surprisingly, when cells were stimulated with EGF on ice, p53 as well as CHC was recruited to the plasma membrane, suggesting that the recruitment of p53 to the plasma membrane occurs in an energy-independent manner (Fig. 3A). A temperature shift to 37 °C induced the internalization of EGFR, in which p53 and CHC were recruited and the rapid dissociation of p53 and CHC from coated vesicles was observed (Fig. 3A). The fluorescent signal from p53 in immunofluorescence was confirmed to be p53 itself by RNAi-directed ablation of p53 expression (Fig. 3B). Similar results were obtained by using different anti-p53 antibodies (DO-1 and pAB421) (Supplementary Fig. S1).

Next, the dynamic distribution of p53 was compared with that of growth factor receptor binding protein 2 (Grb2) or adaptor protein 2 (AP-2), which are involved in the regulation of clathrin-mediated endocytosis of EGFR (Sorkin & Carpenter 1993; Jiang *et al.* 2003). Confocal immunostaining experiments showed that the dynamic behavior of these endocytic regulators upon EGFR activation by EGF was very similar to that of p53 (Fig. 3C,D). When relative values for the localization of p53 and endocytic proteins (CHC, Grb2 and AP-2) at the plasma membrane were quantified, the localization of p53 at the plasma membrane increased approximately 4 times compared with control unstimulated cells (24.1%, EGF treatment; 6.1%, no treatment), while the increased re-location of three endocytic regulators such as CHC (52.2%, EGF treatment; 19.3%, no treatment), Grb2 (36.0%, EGF treatment; 10.2%, no treatment) and AP-2 (35.2%, EGF treatment; 20.6%, no treatment) was also seen upon EGF treatment (Fig. 3E). These results suggest that p53 may serve as a regulator of clathrin-mediated endocytosis. We further examined whether p53 is recruited to the place where EGF forms a complex with EGFR. Treatment of cells with AlexaFluor 488-labeled EGF (AF488-EGF, 2 μg/mL) on ice for 1 h

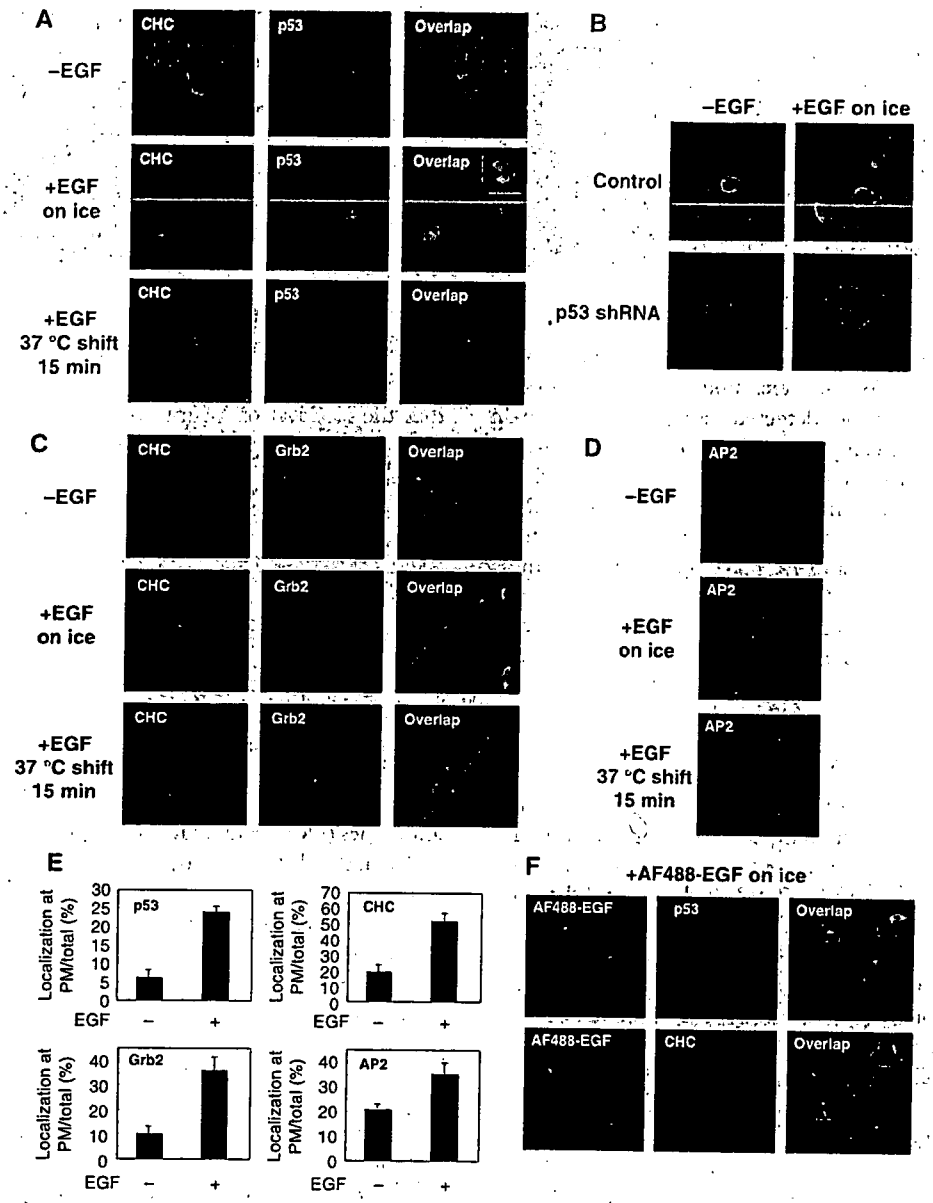

Figure 3 p53 is recruited to the plasma membrane in response to EGF treatment. (A) The localization of CHC (green: AF488 staining) and p53 (red: AF594 staining) in TIG-7 cells was observed by confocal microscopy. Upper panels, untreated cells; middle panels, cells treated with 100 ng/mL EGF for 1 h on ice; bottom panels, cells treated with 100 ng/mL EGF for 1 h on ice followed by rapid warming to 37 °C for 15 min. Insets: Higher magnification images of white rectangles. The co-localization of these proteins is visible as yellow staining. (B) TIG-7 cells stably expressing short-hairpin (shRNA) against p53 were incubated in the absence or presence of EGF (100 ng/mL) for 1 h on ice, fixed with 4% paraformaldehyde and subjected to immunostaining with anti-p53 antibody. (C) TIG-7 cells were treated with EGF as in (A). The localization of CHC (red: AF594 staining) and Grb2 (green: AF488 staining) in TIG-7 cells was observed by confocal microscopy. (D) TIG-7 cells were treated with EGF as in (A). The localization of AP-2 (green: AF488 staining) was observed by confocal microscopy. (E) Quantification of EGF-induced recruitment of p53 and coated proteins to the plasma membrane. The number of cells in which p53 or coated proteins were recruited to the plasma membrane was quantified by cell counting and the percentage was calculated as re-localization at the plasma membrane per total stained cells. (F) p53 co-localizes with EGF–EGFR complex at the plasma membrane. TIG-7 cells were incubated with 2 μg/mL AF488-labeled EGF for 1 h on ice, fixed and subjected to immunostaining with anti-p53 or anti-CHC antibody. Insets: Higher magnification images of white rectangles. The co-localizations of p53 and EGF or CHC and EGF are visible as yellow staining.